Bull. Mater. Sci., Vol. 30, No. 3, June 2007, pp. 271–290. © Indian Academy of Sciences.

Nanowires: properties, applications and synthesis via porous anodic aluminium oxide template

JAYA SARKAR, GOBINDA GOPAL KHAN† and A BASUMALLICK*

Department of Metallurgy and Materials Engineering, †School of Materials Science and Engineering, Bengal Engineering and Science University, Howrah 711 103, India

MS received 10 July 2006; revised 19 April 2007

Abstract. **Quasi one-dimensional nanowires possess unique electrical, electronic, thermoelectrical, optical, magnetic and chemical properties, which are different from that of their parent counterpart. The physical properties of nanowires are influenced by the morphology of the nanowires, diameter dependent band gap, carrier density of states etc. Nanowires hold lot of promises for different applications. Basic electronic devices like junction diodes, transistors, FETs and logic gates can be fabricated by using semiconductor and superlattice nanowires. Thermoelectric cooling system can be fabricated by using metallic nanowires. Semiconductor nanowire junctions can be used for different opto-electronic applications. Moreover, periodic arrays of magnetic nanowires hold high potential for recording media application. Nanowires are also potential candidates for sensor and bio-medical applications.**

In the present article, the physical and chemical properties of nanowires along with their probable applications in different fields have been reviewed in detail. The review also includes highlights of the synthesis of nanowires via porous anodic aluminium oxide template since the technique is simple, cost-effective and a low temperature technique.

Keywords. **Nanowire; properties; quantum-confinement; AAO template; electro-deposition.**

1. Introduction

Recently, nanowires and nanorods of metallic and semiconducting materials have drawn a lot of research interest because of their unique physical properties (Ratner and Ratner 2003; Way 2003), which are interesting from the view point of different device applications. Nanowires have two quantum-confined dimensions and one unconfined dimension. Therefore, the electrical conduction behaviour of nanowires is different from that of their bulk counterpart. In nanowires, electronic conduction takes place both by bulk conduction and through tunneling mechanism. However, due to their high density of electronic state, diameter-dependent band gap, enhanced surface scattering of electrons and phonons, increased excitation binding energy, high surface to volume ratio and large aspect ratio, nanowires of metals and semiconductor exhibit unique electrical, magnetic, optical, thermoelectric and chemical properties compared to their bulk parent counterparts. The interesting properties of nanowires hold lot of promises for applications in the fields of electronics, optics, magnetic medium, thermoelectronic, sensor devices etc (Tonucci *et al* 1992; Whitney *et al* 1993). In view of the interest and immense importance that has been attached to the different properties and applications of nanowires, herein we present a review on the current state of nanowire research. The review aims at highlighting the properties of nanowires and their probable applications in different fields. In addition to this the review also covers in detail the synthesis of nanowires by using porous alumina oxide template.

1.1 *Magnetic properties*

Magnetic nanowire arrays consisting of isolated needle-like magnetic nanowires have recently aroused considerable interest from the viewpoint of perpendicular magnetic recording. The nanowires that are introduced into the pores of alumina template by electrodeposition are potentially capable of producing bit densities in excess of 100 Gbit in^{-2}. When the magnetic field is applied parallel to the long axis of the magnetic nanowire, it exhibits a coercive field, which is inversely proportional to the pore diameter (Chien 1991; Thurn-Albrecht *et al* 2000). It has also been reported that the squareness of the hysteresis loop can be increased from 30% up to nearly 100% by decreasing the wire diameter, D_p.

Figures 1(a) and (b) show the variation of squareness of the hysteresis loop as a function of the applied magnetic

*Author for correspondence
(abasumallick@metal.becs.ac.in, abm@matsc.becs.ac.in)

field (H) parallel and perpendicular to the wire axes for different nanowire diameters. A gradual increase of coercivity is observed with increasing aspect ratio (length (l)/ diameter (d)), but little change is observed when $l/d > 10$ (Skomsk *et al* 2000). Moreover, now it has been established that depending on the geometry, different sites on the surface will differ in local coordination number, which may lead to the variation of moment with local environment (Liu *et al* 1989). Here, it is also important to note that changes in the diameter of the nanowires may influence the surface energies of the different crystallographic planes. It has been reported that in the case of *bcc* α-Fe, the order of surface free energy (γ) for (110), (100) and (111) planes is $\gamma_{110} < \gamma_{100} < \gamma_{111}$, where the values of γ_{110} and γ_{100} are close to each other. However, it has been found that as the diameter of the nanowire increases, the differences in the surface free energy between the crystallographic planes become more significant. Therefore, when nanowires are processed at low temperatures, growth of (110) and (100) planes are nearly equal giving rise to octagonal cross section of the nanowires. At higher temperatures, growth of (110) plane predominates and square shaped nanowires are formed (Aldén *et al* 1994; Vitos *et al* 1998; Spencer *et al* 2002). This change in morphology is expected to cause a change in the magnetization characteristic of the material. Therefore, it is apparent that one can tune the magnetic properties of the nanowires by simply changing their diameter, which will change coercivity, magnetization, remanance and squareness of the hysteresis loop.

It has been found that the total magnetic anisotropy of these nanowires is significantly influenced by the magnetic

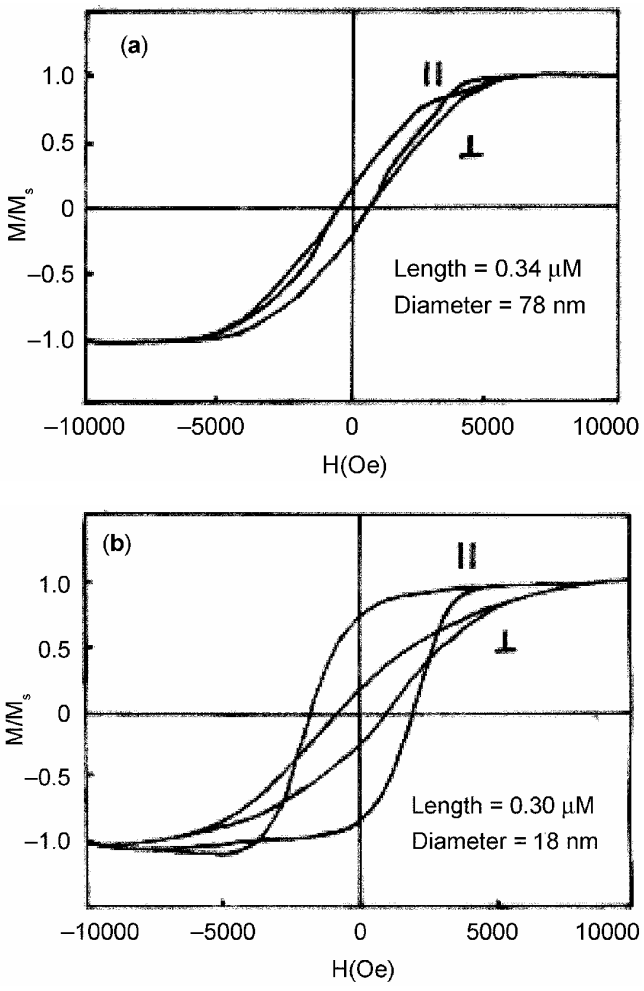

Figure 1. The variation of squareness of hysteresis loops of Co nanowire arrays with applied magnetic field (H) parallel (||) and perpendicular (⊥) to the wire axes: (**a**) nanowire diameter, 78 nm and (**b**) nanowire diameter, 18 nm (Beck *et al* 2005).

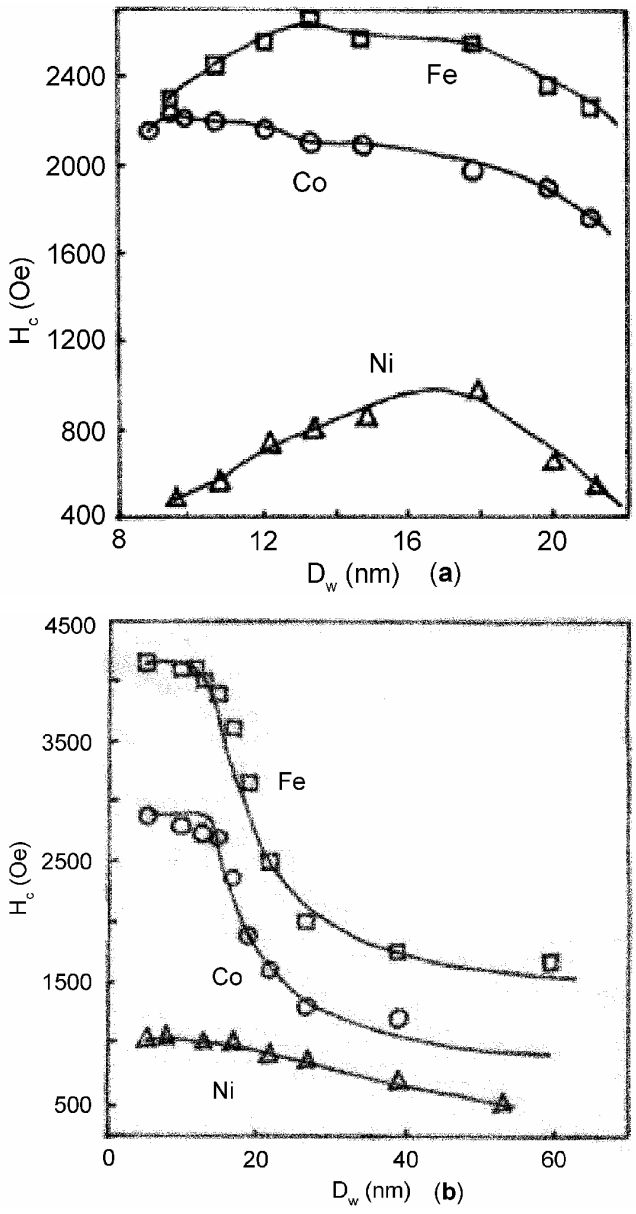

Figure 2. Coercivity as a function of nanowire diameter (D_w) for magnetic nanowires of Fe, Co and Ni at (**a**) room temperature and (**b**) at zero-temperature (Zeng *et al* 2002).

anisotropy, form of the nanowires and the demagnetization fields between the nanowires.

Hexagonally arranged Ni-nanowires embedded in anodic alumina templates have been found to exhibit a strong enhancement in their magnetooptical (MO) response (Peng *et al* 2003). It has been reported (Nielsch *et al* 2001) that the magnetic nanowires of Fe, Co, Ni show much enhanced magnetic coercivity than that of their bulk counterpart. It is important to note that the coercivity is strongly influenced by annealing of the wire at different temperatures, the aspect ratio and the wire diameter. Figures 2(a) and (b) show coercivity of the magnetic Fe, Co and Ni nanowires with their diameters at room temperature and at zero temperature. The temperature dependence of coercivity as a function of wire diameter of Fe nanowires is shown in figure 3(a) and the variation of saturation magnetization as a function of temperature for different diameters of Fe, Co and Ni nanowires are shown in figure 3(b).

Studies on the magnetoresistance (MR) property of nanowires provide a lot of information on the quantization effect, wire boundary scattering of electrons and the effect of doping and annealing on scattering (Heremans *et al* 1998). Zhang *et al* (1998a) studied the MR properties of Bi nanowires in detail. It has been reported (Heremans *et al* 1998, 2000; Zhang *et al* 1998a; Lin and Dresselhaus 2002) that the longitudinal MR, where the magnetic field is applied along the wire axes, the MR peak maxima at a

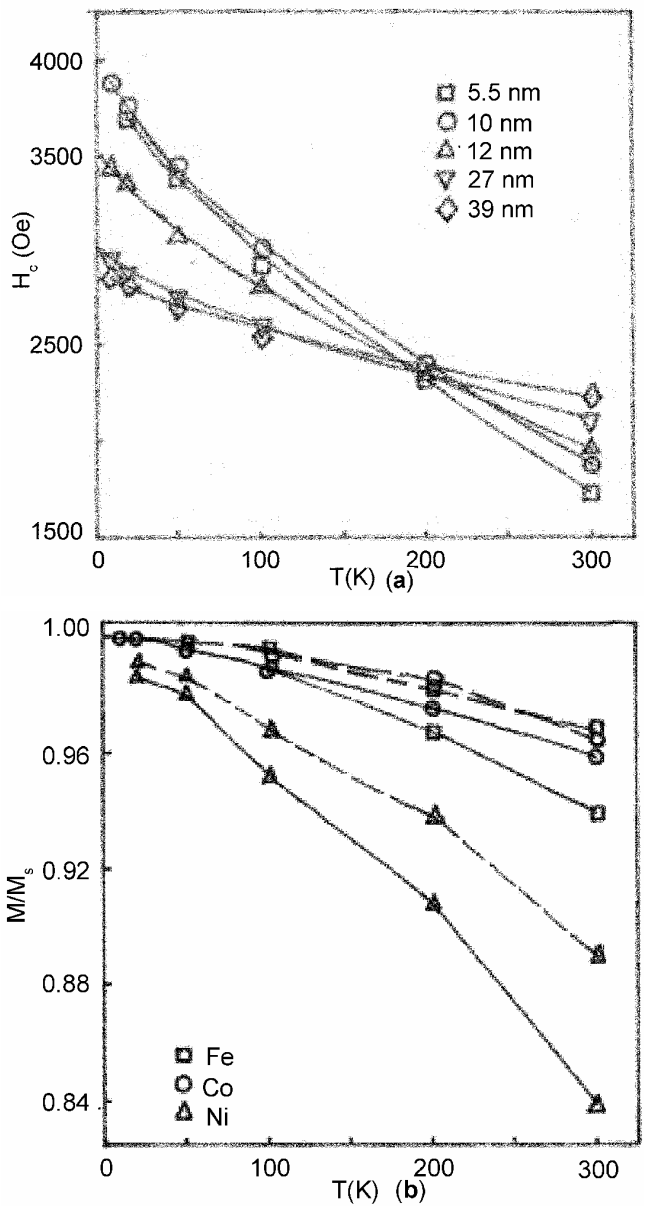

Figure 3. Variation of (**a**) coercivity as a function of temperature with different diameters of Fe nanowires and (**b**) magnetization as a function of temperature for different diameters of Fe, Co and Ni nanowires. (Solid lines: 5·5 nm diameter nanowires, dashed line: 10 nm diameter nanowires (Zeng *et al* 2002)).

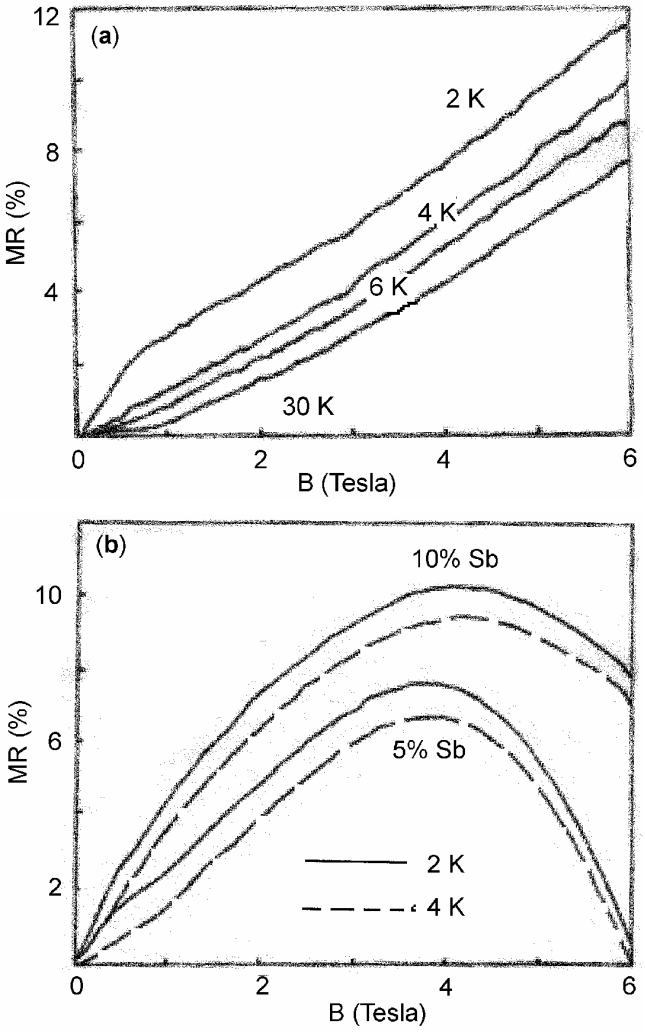

Figure 4. Longitudinal MR of (**a**) 40 nm diameter $Bi_{0.85}Sb_{0.15}$ alloy nanowires and (**b**) 65 nm diameter Bi–Sb alloy nanowires as a function of magnetic field, *B*, at different temperatures (Zhang *et al* 2000).

particular applied field (B) varies linearly with the reciprocal of the wire diameter for a specified temperature. The appearance of the maxima is attributed to the classical size effect. On the other hand, in transverse MR of Bi nanowires, where the magnetic field is applied perpendicular to the wire axis, the temperature follows $T \propto B^2$ in the range of $0 \leq B \leq 5{\cdot}5T$.

It has been found that the MR of nanowires is highly diameter dependent. The longitudinal MR as a function of magnetic field for $Bi_{0{\cdot}85}Sb_{0{\cdot}15}$ alloy nanowires with 40 nm diameter at different temperatures are quite linear as shown in figure 4(a). On the other hand, 65 nm diameter $Bi_{1-x}Sb_x$ nanowires exhibit different types of longitudinal MR as a function of the applied field as can be seen in figure 4(b). The maxima in MR are attributed to the boundary scattering effect (Zhang *et al* 2000).

It has been reported (Heremans *et al* 1998) that the 1-D confined system at low magnetic field can be transformed into 3-D confined system by applying a longitudinal magnetic field to the nanowire arrays at very low temperatures. The Bi nanowires of diameter up to 200 nm show the Shubnikow-de Hass (SdH) oscillating effect, which appears because of the field strength variation when the quantized Landau level passes through the Fermi energy level (Heremans and Thrush 1999).

1.1a *Applications*: The most attractive potential applications of nanowires lie in the magnetic information storage medium. Studies have shown that periodic arrays of magnetic nanowire arrays possess the capability of storing 10^{12} bits/in^2 of information per square inch of area. The small diameter, single domain nanowires of Ni, Co fabricated into the pores of porous anodic alumina (Thurn-Albrecht *et al* 2000; Nielsch *et al* 2001) has been found to be most suitable for the above purpose. The high aspect ratio of the nanowires results in enhanced coercivity and suppresses the onset of the 'superparamagnetic limit', which is considered to be very important for preventing the loss of magnetically recorded information between the nanowires. Suitable separation between the nanowires is maintained to avoid the inter-wire interaction and magnetic dipolar coupling. It has been found that nanowires can be used to fabricate stable magnetic medium with packing density $> 10^{11}$ wires/cm^2.

1.2 *Thermoelectric properties*

Nanowires exhibit interesting thermoelectric properties. The unique electronic band structure and diameter dependent variation in electron density of state make nanowires promising materials for various thermoelectronic applications (Hicks and Dresselhaus 1993; Heremans *et al* 1998). Metal nanowires exhibit many fold increase in Seebeck coefficient due to their enhanced density of electronic states at the one-dimensional sub-band edges, which is attributed to the quantum confinement effect. Here it would be worthwhile to mention that the thermopower of the metallic nanowires also increases because of the enhanced electronic density of state near the Fermi energy level. Studies have shown that the Seebeck coefficient and thermopower of metallic nanowires are significantly influenced by the wire diameter and the alloy phase concentration. It is also observed that the thermal conductivity of nanowires is influenced by the wire diameter. The variations of thermal conductivity (k) as a function of temperature for Si nanowires of different diameters are shown in figure 5.

It has been reported (Heremans *et al* 2002; Lin *et al* 2002) that in Sb and Si doped Bi nanowires, the thermopower can be increased by decreasing the wire diameter. A similar phenomenon has also been observed in case of alumina doped Zn nanowires (Heremans *et al* 2002). Bi nanowires also exhibit significant temperature (T) dependence of resistance, $R(T)$, and the phenomena is strongly influenced by the variation of diameter of the nanowires (Heremans *et al* 2000). Here it should be noted that the Bi nanowires exhibit quantum confinement effect below certain critical diameter (~ 48 nm) and the semimetallic phase of Bi transforms into the semiconducting phase (Heremans *et al* 2000, 2002; Lin *et al* 2000). This phenomenon implies that at elevated temperature or at room temperature, the semimetallic phase transformation of Bi nanowires is possible only by reducing the wire diameter. The crystalline structure of the material is also an important factor, which influences the quantum size effect of nanowires. In polycrystalline nanowires, the resistance maxima that can

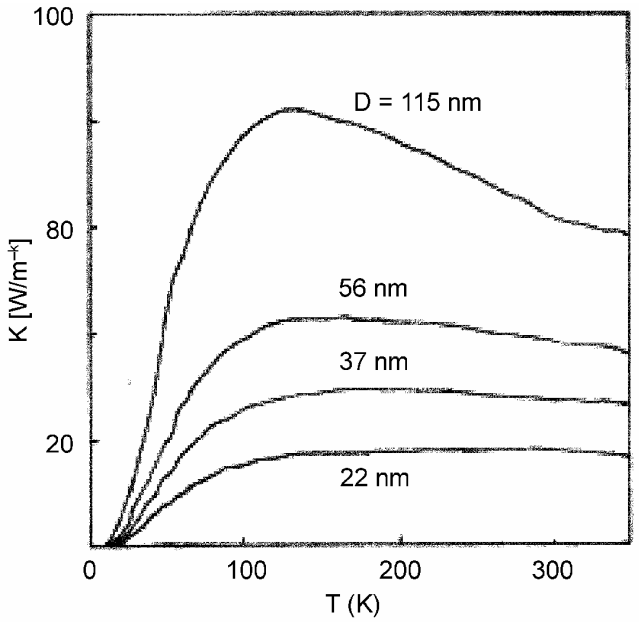

Figure 5. Thermal conductivity (k) as a function of temperature for Si nanowires of different diameters (D) (Dames and Chen 2002).

be normally observed in $R(T)$ vs T curve is not observed because of less carrier mobility due to the boundary scattering effect (Lin *et al* 2002). Plots of $R(T)/R$ (270 K) ratio measured as a function of temperature, $T(K)$, for 40 nm Bi and Te doped Bi nanowires are shown in figure 6(a). The average carrier mobility ratio, $\mu(T)/\mu$ (270 K), for the same nanowires were also calculated from the $R(T)$ value and the T-dependent carrier density measurement. Figure 6(b) shows the temperature dependence of mobility ratio, μ (270 K)/μ (T), where N_d stands for the doped Te ion concentration (ions/cm^3).

Investigations have clearly shown that the electronic wave function becomes more localized with the reduction of diameter of the nanowires (Beutler and Giordano 1988; Venkatasubramanian *et al* 2001; Heremans *et al* 2002). This phenomenon is considered to be the key factor that causes nanowires to exhibit interesting thermoelectric properties.

1.2a *Applications*: The enhanced thermopower and manyfold increase in the Seebeck coefficient of nanowires make them very attractive for thermoelectric cooling system and energy conversion devices (Dresselhaus *et al* 1998; Chen *et al* 2003).

1.3 *Electrical properties (transport properties)*

Electron transport properties of nanowires are very important for electrical and electronic applications as well as for understanding the unique one-dimensional carrier transport mechanism. It has been noticed that the wire diameter, wire surface condition, crystal structure and its

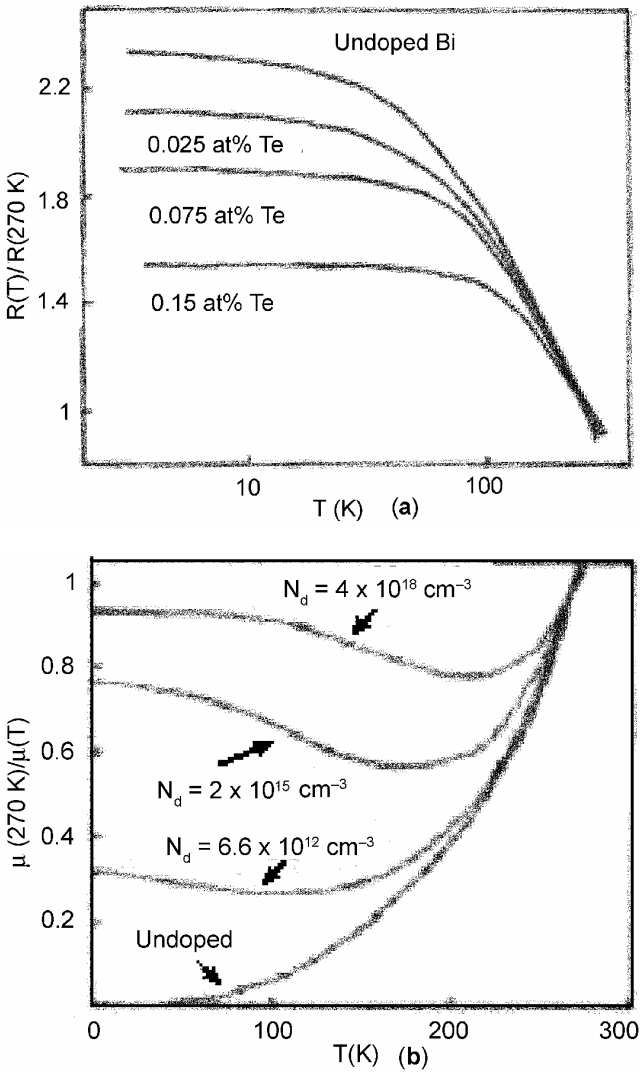

Figure 6. (**a**) The $R(T)/R$ (270 K) of 40 nm diameter Bi nanowires with different amounts of Te alloy concentrations (Lin *et al* 2000) and (**b**) carrier mobility ratio as a function of temperature of 40 nm Bi nanowires with different doped Te atom concentration (Lin *et al* 2000).

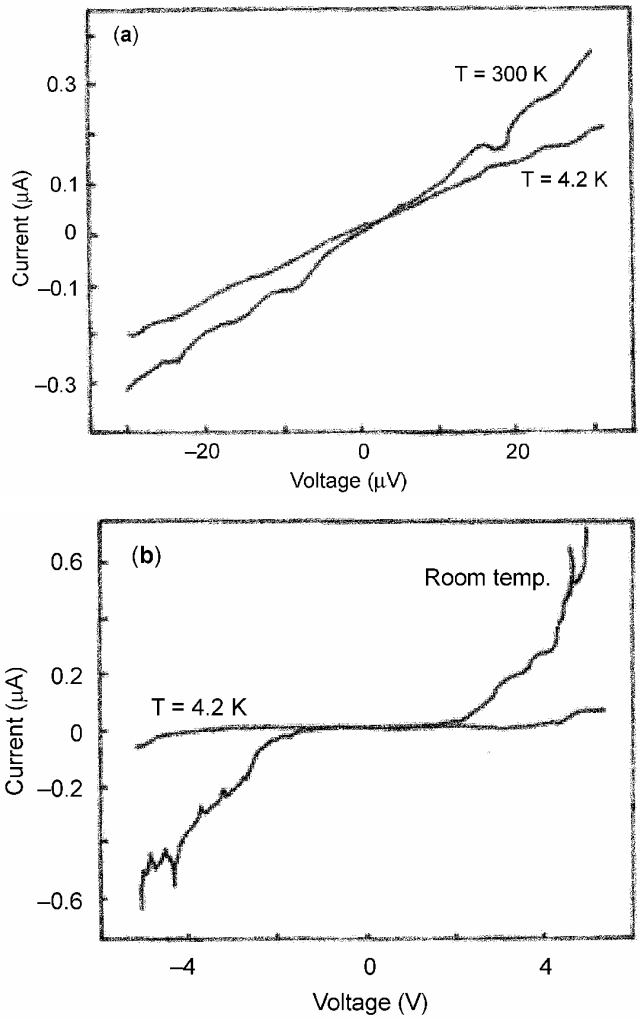

Figure 7. (**a**) I–V characteristics of the metallic Cu nanowire at 4·2 K and at room temperature and (**b**) I–V curves of the wire at 4·2 K and room temperature recorded after oxidation of Cu nanowires (Molaresa *et al* 2003).

quality, chemical composition, crystallographic orientation along the wire axis etc are important parameters, which influence the electron transport mechanism of nanowires. Figure 7(a) shows the *I–V* characteristics of the Cu nanowires both at room temperature and at 4·2 K. The plot clearly shows the linear ohmic behaviour. However, by oxidation when the metallic Cu nanowires are transformed into semiconducting Cu_2O nanowires and placed between two electrodes, it forms two Schottky diodes in series and a double diode like *I–V* characteristic curve is obtained as shown in figure 7(b).

It has been reported that quasi one-dimensional nanowires exhibit both ballistic and diffusive type electron transport mechanism, which depends upon the wire length and diameter. Ballistic type transport phenomena is associated with predominant carrier flow without scattering which is due to the fact that the carrier mean free path is longer than that of the wire length (Bhushan 2005). Ballistic type transport mechanism is normally observed at the contact junction of nanowire and other external circuits (Muller *et al* 1992, 1996), where the conductance is quantized into an integral multiple of $2e^2/h$, called the universal conductance unit (e is the electronic charge and h the Plank's constant) (van Wees *et al* 1988; Wharam *et al* 1988).

In the case of ballistic type transport in metallic nanowires, the conductance quantization phenomena takes place because of the fact that the nanowire diameter becomes comparable to the electron Fermi wavelength of that metal (Costa-Krämer *et al* 1997). As compared to the ballistic transport mechanism, in diffusive type conduction mechanism, the carrier mean free path is smaller than that of the wire length. Therefore, various types of scattering affect the carriers and the carrier transport mechanism of nanowires becomes quite similar to that of bulk counterpart.

The clearest view of the electron transport mechanism of the metallic and semiconducting nanowires can be easily obtained by considering three parameters viz. wire diameter (d), carrier mean free path (l_c) and the de Broglie wavelength of electron (λ_e). Earlier studies have shown that when the wire diameter (d) is larger than the carrier mean free path (l_c) and the de Broglie wavelength of electron (λ_e) i.e. $d >> l_c$ and $d >> \lambda_e$, the electron transport mechanism of nanowires remains similar to that of bulk counterpart. However, if the wire diameter (d) becomes smaller or comparable to that of the carrier mean free path (l_c) and much larger than the de Broglie wavelength of electron (λ_e) i.e. $d \leq l_c$ and $d >> \lambda_e$, the electron transport mechanism of nanowires follows the classical laws of physics. On the other hand, when the carrier mean free path (l_c) and the de Broglie wave length of electron (λ_e) both become comparable to the wire diameter i.e. $d \leq l_c$ and $d \sim \lambda_e$, the phenomena of quantum confinement occurs in nanowires which includes significant change in the density of electron states. Studies show that the electronic density of states (DOSs) of nanowires is strongly diameter dependent. For example, electronic DOSs of Ti nanowires of diameter < 1 nm exhibit some discrete peaks like molecules as shown in figures 8(a) and (b). Thicker Ti nanowires (diameter, > 1 nm) show bulk Ti like electronic DOSs, because of the formation of continuous electronic bands caused by the overlapping of discrete molecular levels with each other as shown in figures 8(c) and (d).

However, it is found that the conductance of nanowires strongly depends on their crystalline structure. For example, in the case of perfect crystalline Si nanowires having four atoms per unit cell, generally three conductance channels are found (Zhao *et al* 2003). One- or two-atom defect, either by addition or removal of one or two atoms may disrupt the number of such conductance channel and may cause variation in the conductance. Variation in conductance due to the above reason is shown in figure 9, where conductance is plotted as a function of energy for perfect Si nanowires and single atom addition defect nanowire.

It is to be noted that change in the surface conditions of the nanowires can cause remarkable change in the transport behaviour. This has been illustrated in figure 10, where it can be seen that change in electrical conductivity has been caused by the variation of the surface scattering phenomena of carriers in nanowires, when the diameters of the nanowires are changed.

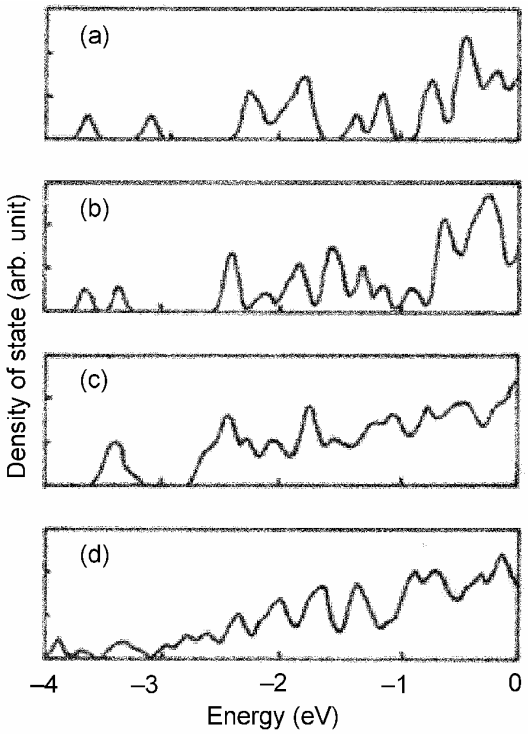

Figure 8. Electronic densities of states (DOSs) of Ti nanowires: (**a**) and (**b**) wire diameter < 1 nm and (**c**) and (**d**) wire diameter >1 nm with 0·05 eV Gaussian broadening. The Fermi level is set as zero on the energy axis (Wang *et al* 2001).

It has also been reported (Duan *et al* 2002) that the redox molecules like cobalt phthalocyanine layer coating on the *n*-InP nanowires change their conductance remarkably. Researchers have shown that the resistance of Pd nanowires changes by an order of magnitude due to the adsorption of hydrogen gas molecules on the wire surface.

Recently, electron transport mechanism of superlattice nanowires has acquired lot of interest because of their potential applications in thermoelectronics (Lin and Dresselhaus 2003), nanobarcodes (Wu *et al* 2002), nanolasers (Gudiksen *et al* 2002), one-dimensional waveguide and resonant tunneling diodes (Björk *et al* 2002a, b). Superlattice nanowires consist of periodic modulation of chemical composition and crystal structure in the form of quantum dots along the wire axes. The electron transport phenomena between those quantum dots are governed by the quantum tunneling mechanism in which specific regions of the nanowires with a particular composition act as the potential barrier. As for example, in case of the InAs–InP superlattice nanowires the InP dots act as the potential barrier (Björk *et al* 2002a, b). It is to be noted that the interfaces between the quantum dots have the capability of blocking the phonon conduction along the wire axes without affecting the electrical conduction.

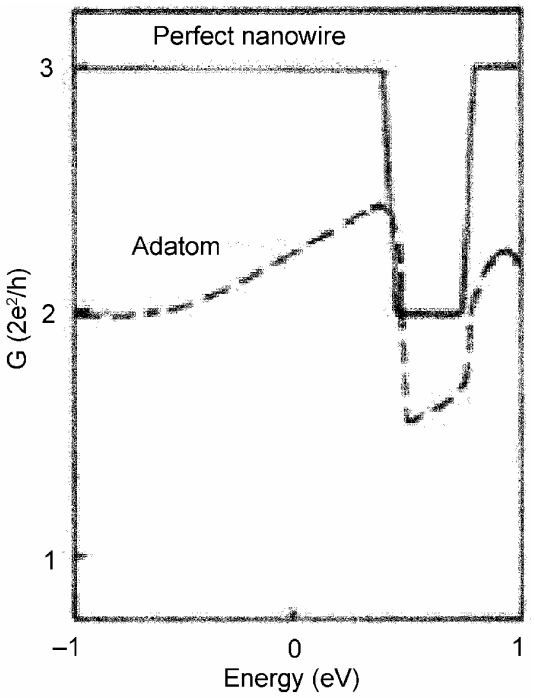

Figure 9. Conductance, $G(2e^2/h)$ of silver nanowires with single-atom defects: Adatom (dotted line) and for perfect nanowires (solid curve) (Zhao *et al* 2003).

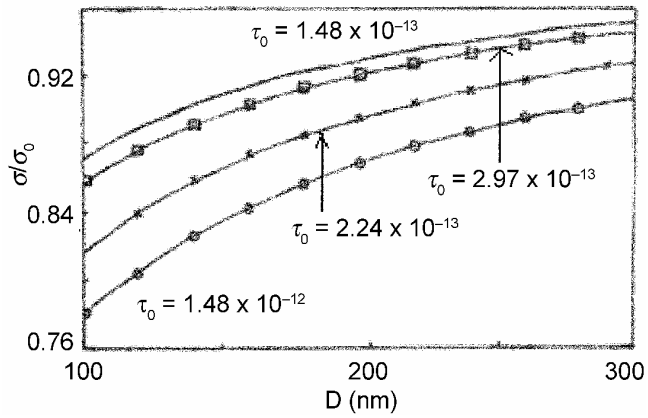

Figure 10. Relative conductivity vs nanowire radius (D), at 300 K, where σ_0 is the bulk conductivity corresponding to scattering time, τ_0 (in s) (Redwing *et al* 2002).

1.3a *Applications*: Nanowires possess the potential for use in numerous electronic applications. Junctions of semiconductor nanowires such as GaAs and GaP have shown good rectifying characteristics (Gudiksen *et al* 2002). Several semiconductor devices such as junction diodes (Huang *et al* 2001; Kim *et al* 2002), memory cells and switches (Duan *et al* 2002), transistors, FETs (Huang *et al* 2001; Duan *et al* 2002), LEDs (Duan *et al* 2001; Gudiksen *et al* 2002) and inverter (Derycke *et al* 2001) etc have already been fabricated using nanowire junctions. Figure 11(a) shows a schematic diagram of FET made of nanowires. The LED fabricated by a crossed junction of *p*-Si and *n*-GaN with their *I–V* characteristics and EL spectra are shown in figures 11(b) and (c), respectively. These basic building blocks of semiconductor devices can be used to fabricate complex IC chips of much reduced dimension.

It has been found that these junction devices exhibit transport and current rectifying properties similar to their parent counterpart. Several attempts have been made to fabricate nanowire diode and it has been demonstrated that the crossings of phosphorus (*n*) and boron (*p*) doped Si nanowires form *p–n* junction diodes (Cui *et al* 2001). Similar type of junction diode can also be formed by *n* and *p* type InP nanowires (Duan *et al* 2001). Figures 12(a) and (b) show an in-plane gate (IPG) quantum wire transistor (QWRTr) and a warp gate (WPG) quantum wire transistor made of GaAs nanowires, respectively. A WPG QWR-based binary decision diagram (BDD) device is shown in figure 12(c) and figure 12(d) represents the SEM image of hexagonal BDD 2 bit digital Adder circuit.

The field effect transistors made of nanowires exhibit remarkably modified conductance behaviour (Chung *et al* 2000; Cui *et al* 2000; Huang *et al* 2002) and they are very attractive because of their morphological advantages. The operational speed of FETs made of nanowires is much faster compared to that of bulk FETs.

In contrast to the crossing of two distinctive nanowires, several heterogeneous junctions can be formed inside single superlattice nanowire, by varying the materials

compositions along the wire axes (Gudiksen *et al* 2002) or perpendicular to the wire axes (Lauhonn *et al* 2002).

Nanowire junctions can also perform certain logical operations and can be used as logic gates (Huang *et al* 2001; Duan *et al* 2002) (see figure 13). The electroluminescence (EL) properties of nanowires can be employed for different opto-electronic applications (Duan *et al* 2001). For example, figure 14(a) represents three crossed junctions made of *p*-Si nanowire with *n*-GaN, *n*-CdS and *n*-CdSe nanowires and their corresponding EL spectral peak (figure 14(b)).

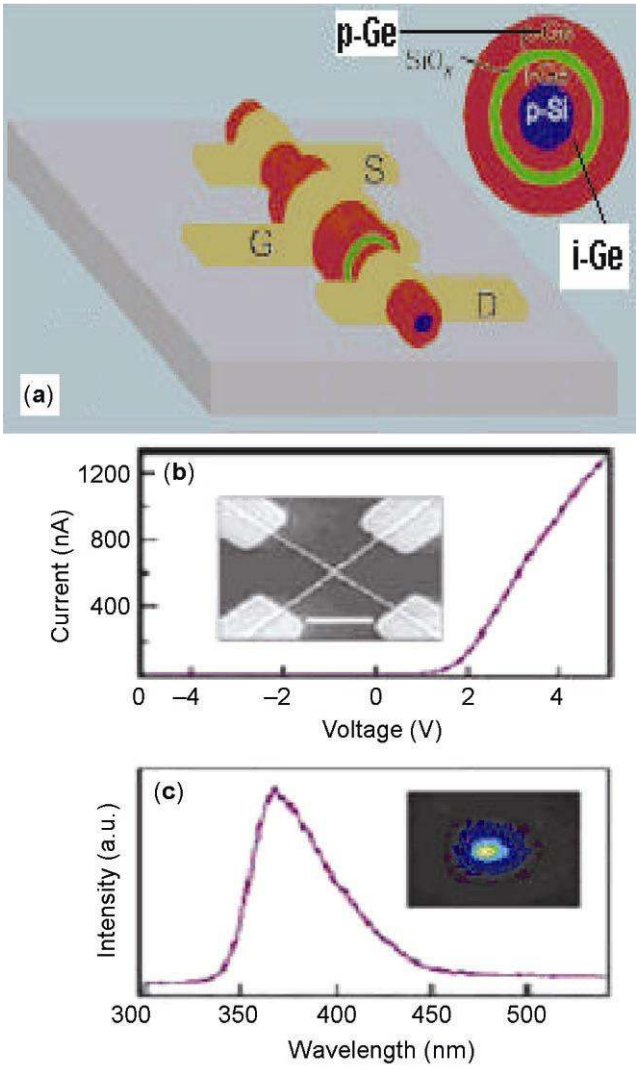

Figure 11. (**a**) Schematic representation of a coaxially fabricated nanowire FET. Inset: Cross sectional view of FET with layers of *i*-Ge (red, 10 nm), SiO_2 (green, 4 nm), and *p*-Ge (5 nm). The source (*S*), drain (*D*) and gate (*G*) electrodes are also shown, (**b**) *I–V* characteristics of a *p*-Si/*n*-GaN crossed junction LED. Inset: Scanning electron microscopic (SEM) image of the junction LED (Huang *et al* 2005) and (**c**) EL spectra of the LED. Inset: EL image representing the spatial of intensity having a maximum at the crossed junction (Huang *et al* 2005).

Nanowire arrays can be used in field emission devices such as flat panel displays (Ding *et al* 1999) because of the significant drop in the work function of the surface electrons in those small diameter and high curvature tips of the nanowires (Au *et al* 1999).

1.4 *Optical properties*

The optical properties of nanowires have been studied extensively by employing different optical characterization and analytical techniques. The complex dielectric function ($\varepsilon_1 + \varepsilon_2$) of the nanowires which are embedded in the host material are deduced with the help of effective medium theories (Garnett 1906; Aspnes 1982; Cardona 1982; Yu and Cardona 1995) by considering the nanowires and the host matrix to act as a single material. The refractive index (n) and the absorption coefficient (k) of the medium are related to ε_1 and ε_2, respectively for the composite medium. The complex dielectric function of the nanowires can also be determined directly with the help of standard reflection and transmission measurements combined with Maxwell's equations (Black *et al* 2002). The band gap and temperature variation of band gap of the nanowires can be determined from the complex refractive index measurements (Lee *et al* 2001), which are considered to be important parameters for selection of materials for particular photonic applications. Information about plasmon frequency, donor atom concentration and carrier concentration of nanowires can be obtained by analysing the infrared (IR) spectra of the nanowires.

Metallic nanowires exhibit interesting plasmon absorption effect. Research has shown that the energy of the surface plasmon band is sensitive to various factors such as particle size, shape, composition, surrounding media and inter particle interactions (Kerker 1969; Bohreu and Huffman 1983; Foss *et al* 1994; Schider *et al* 2001). It has been reported that changeover from spherical to rod shaped nanostructure of Ag leads to splitting from an original single absorption band to two absorption bands that separate and become very prominent with increasing aspect ratio (Bohreu and Huffman 1983). It has also been found that single crystal Ag nanowire arrays with high aspect ratio exhibit two plasmon absorption bands as shown in figure 15. The first peak arises due to the transverse plasmon resonance and the second peak is attributed to the longitudinal plasmon resonance (Foss *et al* 1994; Huang *et al* 1996). Studies on the surface plasmon modes on Ag and Au nanowires have shown the occurrence of multipolar plasmon resonances, which can be explained by the standing plasmon wave considerations (Schider *et al* 2003). Recently, it has been reported that multiple peaks appear in the plasmon absorption spectra of the sulfide coated gold nanorods (Chatterjee *et al* 2006).

The photoluminescence (PL) spectroscopic studies on semiconducting nanowires (InP, CdS, ZnO nanowires)

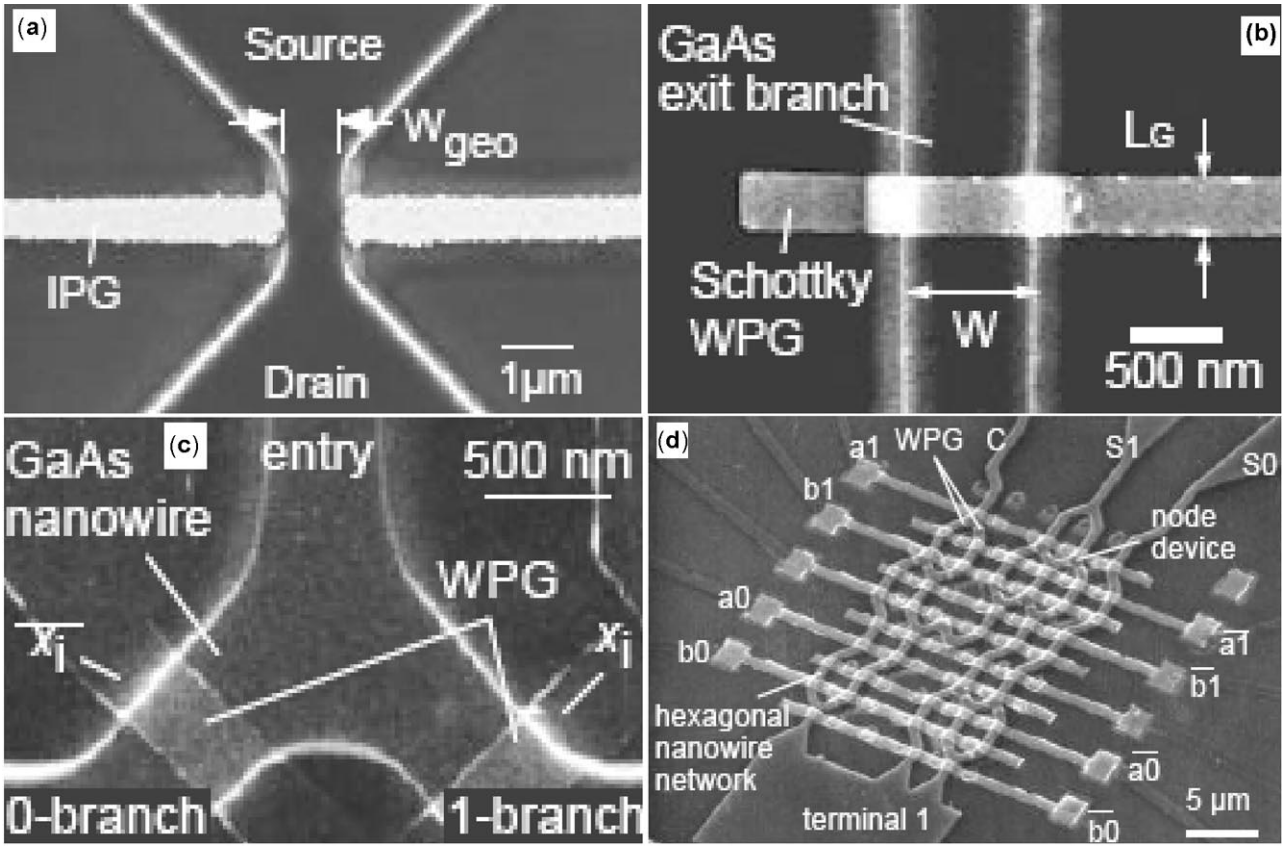

Figure 12. SEM image of (**a**) IPG QWRTr, (**b**) WPG QWRTr, (**c**) WPG QWR-based BDD device and (**d**) hexagonal BDD 2 bit digital adder (Hasegawa 2001).

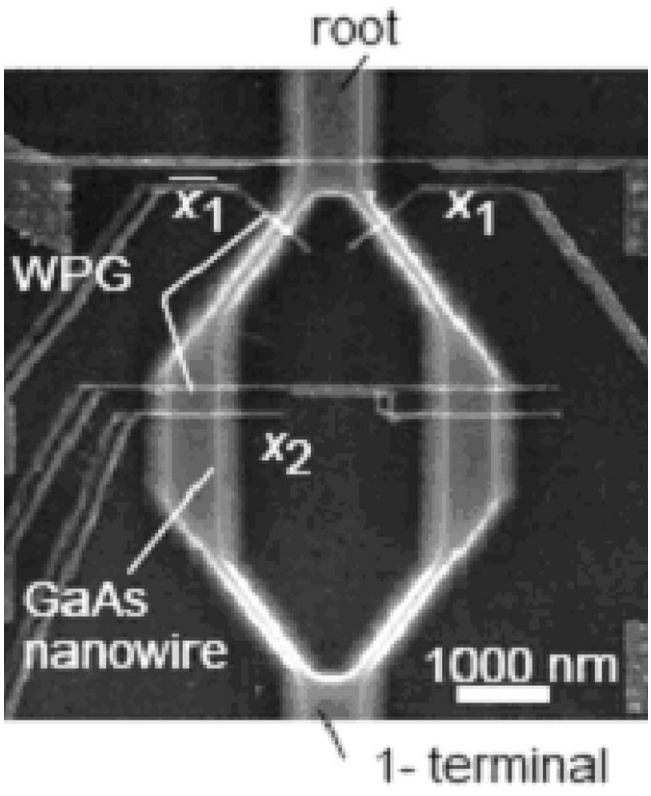

Figure 13. SEM image of a WPG single electron BDD OR logic gate (Hasegawa 2001).

(van Vugt *et al* 2005) have shown that the PL energy peak and band gap increases with the decrease of the wire diameter. The above phenomena confirm the effect of quantum confinement in nanowires when the wire diameter is reduced.

Fluorescence study of nanowires provides vivid information about the band gap, quantum confinement effect, strain in nanowires, oxygen vacancies, electron effective masses and Fermi energies (Gudiksen *et al* 2002; Lyons *et al* 2002; Zheng *et al* 2002). The number of subbands of the nanowires can be measured with the help of magneto-optic techniques. The determination of the number of subbands in nanowires is very important for determining the electron transport properties in them (Blom *et al* 1998). It is to be noted that magnetic properties of the nanowires can also be determined by the above-mentioned techniques (Sugawara *et al* 1997; Pierce *et al* 2002).

Figures 16(a) and (b) show the magneto-optical (MO) spectra of different diameter Ni nanowires. The magneto-optical polar rotation (Kerr rotation) spectra as shown in figure 16(a) reveals that arrays of 35 nm diameter Ni nanowires exhibit sharp peak like bulk Ni around 3·4 eV, due to an enhancement in the polar rotation. Figure 16(b) shows the corresponding zero magnetic field reflectivity ($\Delta R/R$) of the nanowires.

Nanowire arrays exhibit non-linear optical properties, which make them very attractive for application as photonic

material. The sharp increase in the energy of the absorption peak with the decrease of the wire diameter is attributed to quantum confinement effect (Lin *et al* 2000) and the occurrence of the blue shift. The extinction spectra of silver nanowires with different diameters shown in figure 17, revealed that for fixed length (h) of the nanowires when the diameter (d) decreases, λ shifts towards the shorter wavelength side because of the quantum confinement effect.

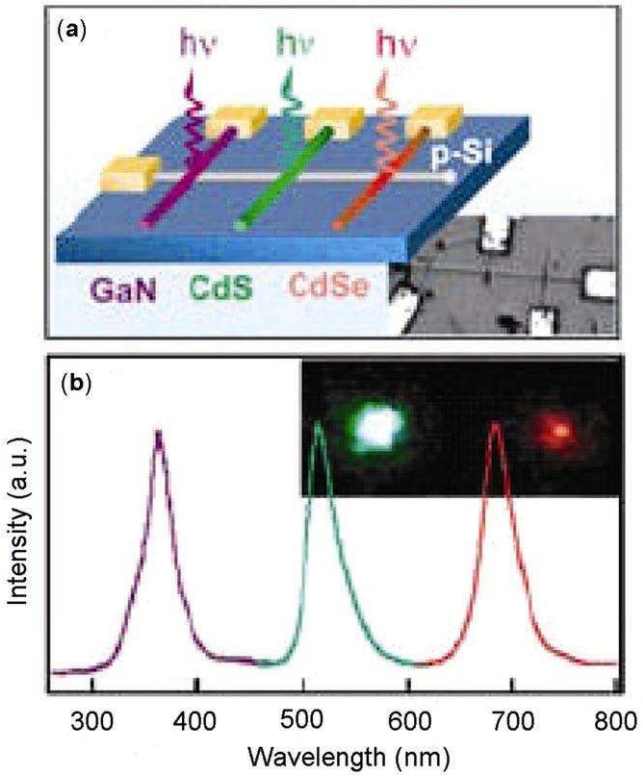

Figure 14. (**a**) Schematic representation of three crossed junction diodes made of different nanowires. Inset: SEM image of the junction is shown and (**b**) corresponding EL spectrum from the three junctions are shown (Huang *et al* 2005).

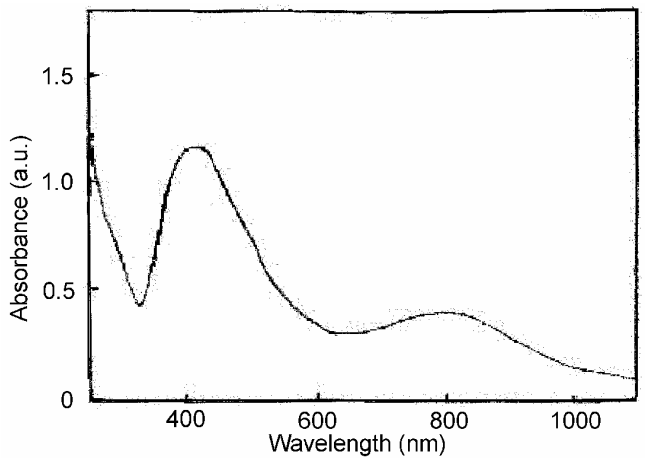

Figure 15. Two plasmon absorption peaks for Ag nanowires (Jiang *et al* 2001).

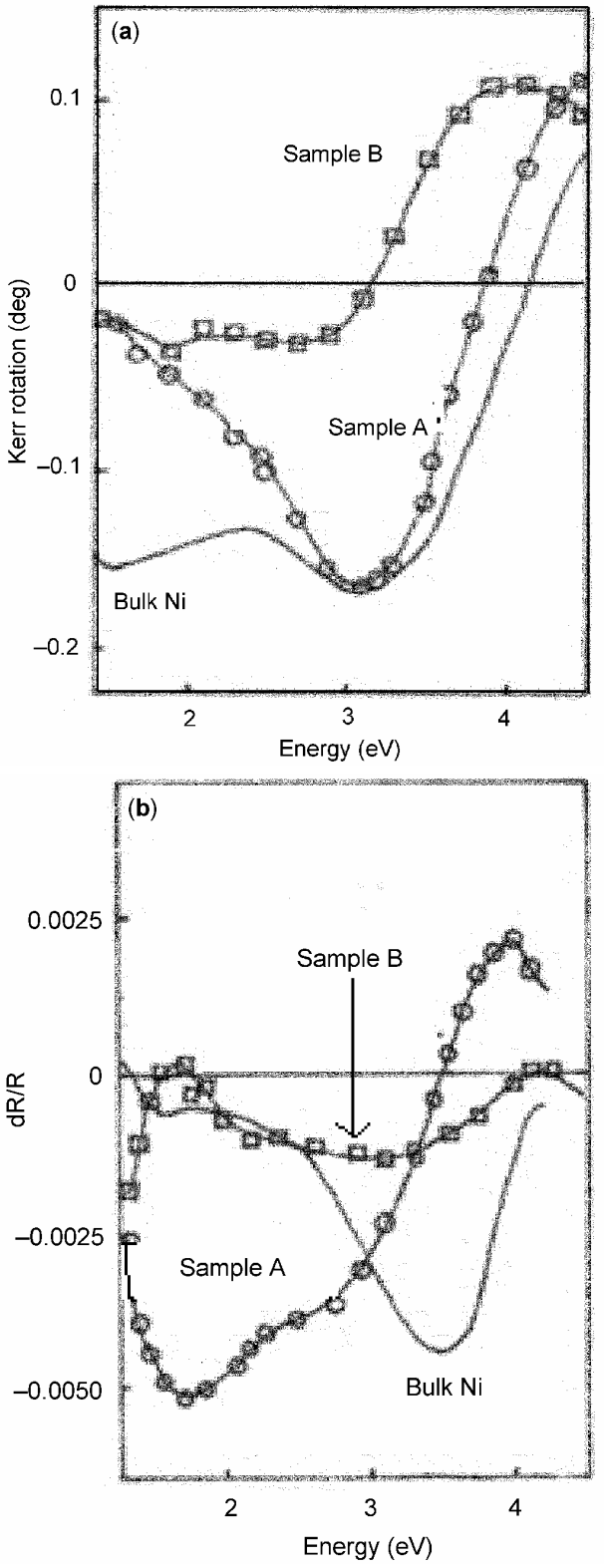

Figure 16. MO polar (**a**) Kerr spectra and (**b**) reflectivity comparison between Ni nanowires array and bulk Ni. Samples A and B represent nanowires with diameters 35 nm and 180 nm, respectively (Melle *et al* 2003).

1.4a *Applications*: Uniform morphology and interesting optical properties of nanowires have raised their potential for various optical applications. The *n–p* junction of nanowires has been found to be capable of light emission, by virtue of their photoluminescence (PL) or electroluminescence (EL) properties. The use of *p–n* junction nanowires has been contemplated for laser applications. It has been established that ZnO nanowires of wire diameter smaller than the wavelength of emitted light exhibits lasing actions (Huang *et al* 2001a; Johnson *et al* 2002) at lower threshold energy compared to their bulk counterpart. This has been attributed to the exciton confinement effect in the laser action, which decreases the threshold lasing energy in nanowires. This effect has been observed in small diameter ZnO (385 nm diameter) and GaN nanowires (Johnson *et al* 2001, 2002).

The *n–p* junction nanowires or superlattice nanowires with *p–n* junctions can also be used as light emitting diodes (Duan *et al* 2001; Zhao *et al* 2003). The huge surface area and the high conductivity along the length of nanowires are suitable for inorganic–organic solar cell (Huynh *et al* 2002). The solar cell made of CdSe nanowires has high efficiency (Wu *et al* 2002). Very recently the sub-wavelength diameter Si nanowires have been used as low-loss optical waveguides within visible to near-IR range of spectrum. Studies have shown that the optical losses of those Si sub-wavelength diameter nanowires are much lower compared to that of other sub-wavelength diameter metallic plasmon waveguides (Takahara *et al* 1997; Maier *et al* 2002, 2003). The optical loss of different diameter Si nanowires transmitting the wavelength of 633 nm and 1550 nm are shown in figure 18(a) and figure 18(b) represents a SEM image of a coiled 260 nm diameter Si nanowire of nearly 4 mm in length.

Nanowires made of various metal segments like Ag, Au, Ni, Pd etc can be used as barcode tags (Nicewarner *et al* 2004) for different optical read outs.

It is to be noted that when the intensity of the incident photons are increased the electron density of the subband edges also increases, due to the above fact, these quantum wires develop strong nonlinearity. Therefore, nanowires may be used to develop optical switches. These optical switches will be able to operate at lower energy and with enhanced switching speed compared to the known switches.

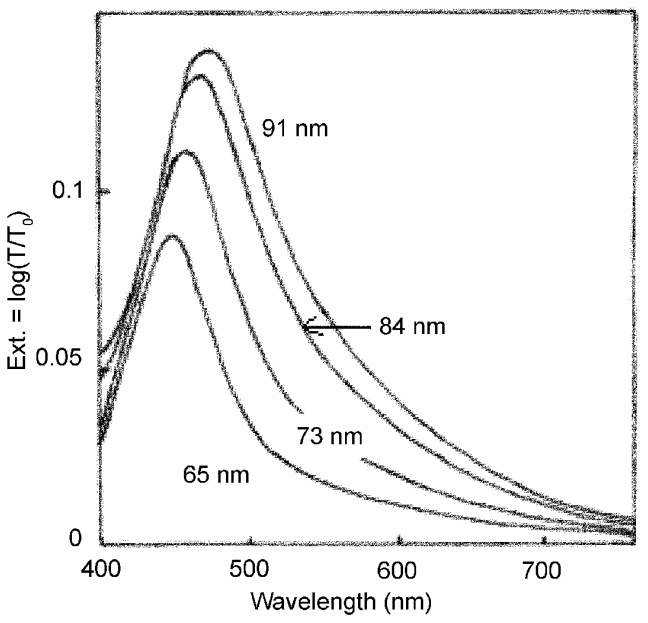

Figure 17. The extinction spectra of different diameter Ag nanowires are shown. The electric field of the incident light is perpendicular to the wire axes. In this plot h = 50 nm, d varies from 65–91 nm and Λ = 840 nm (Schider *et al* 2001).

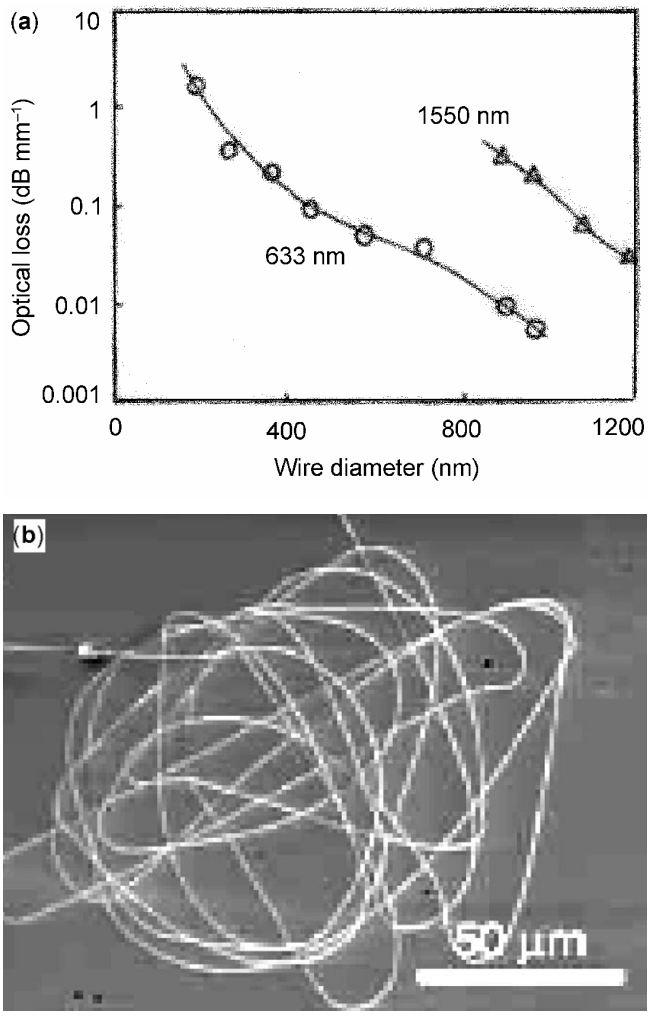

Figure 18. (**a**) Optical loss of silica wires measured at a wavelength of 633 nm (filled dark circles) and 1550 nm (unfilled white circles) (Nicewarner *et al* 2004) and (**b**) SEM image of a coiled 260 nm diameter Si nanowires of length of nearly 4 mm (Tong *et al* 2003).

1.5 *Chemical properties*

Nanowires also exhibit interesting chemical properties mainly because of their enhanced surface to volume ratio, high aspect ratio, large curvature at the nanowire tips and huge number of surface atoms. The high chemical reactivity, interesting electrical and electronic properties of nanowires make them very attractive for sensor devices applications. Figure 19 shows an Au/Pt/Au nanowire with a butaneisonitrile monolayer adsorbed on the wire surface. It is to be noted that all the butaneisonitrile molecules adsorbed to the Au part of the nanowire can only be replaced by 2-mercaptoethylamine (MEA) when the wire is exposed to MEA because of the enhanced chemical reactivity of Au over Pt.

Chemical and biological sensors made of nanowires as sensing probe exhibit enhanced sensitivity and fast responsivity compared to the conventional sensors, as they need less electrical power to work. It is believed that the capability of providing real space-time distribution of a particular species will be improved significantly if arrays of nanowires are used in the sensing probe. These types of nanowire sensors can also estimate the real concentration of a particular substance quickly. It should be noted that functioning of nanowire-based sensors is based on the principle of change in electrical conductivity, which arises due to the adsorption of the molecules that are required to be detected. This has been illustrated in figure 20,

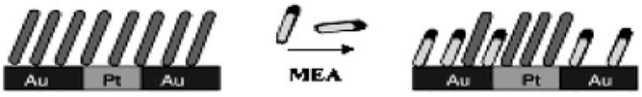

Figure 19. Schematic of an Au/Pt/Au nanowire with a butaneisonitrile monolayer replaced by MEA from all the Au part of the nanowire (Wanekaya *et al* 2006).

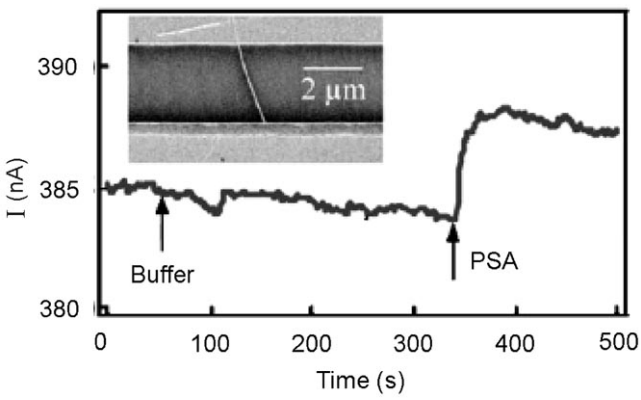

Figure 20. The curve represents the change in current as a function of time for an individual In_2O_3 nanowire when exposed to buffer and PSA. Inset: SEM image of the single In_2O_3 nanowire sensor device is shown (Wanekaya *et al* 2006).

where the electrical current as a function of time, plotted for In_2O_3 nanowires clearly shows enhancement in current when the protein specific antigen (PSA) molecules are adsorbed on the wire surface. Considering the fact that fast and accurate detection of various biological compounds is a primary necessity for medical diagnosis, nanowire based sensors definitely hold a lot of promise in this area.

1.5a *Applications*: The development of nanowire based pH sensor (Cui *et al* 2001) and Pb nanowire based hydrogen gas sensor (Favier *et al* 2001) have been reported so far.

2. Synthesis of nanowires via porous anodic aluminium oxide template

Research works, which are focused on the realization of the potential benefits of nanowires, have incidentally led to the development of a large number of fabrication techniques. Some of the important methods are ion beam and electron beam nanolithography (Chou *et al* 1994; Dunn 1994; Hehn *et al* 1995; Cerrina and Marrian 1996; Matsui and Ochiai 1996; Gibson 1997), evaporation–condensation (Liu *et al* 2001), vapour–liquid–solid (VLS) growth (Wu and Yang 2000; Huang *et al* 2001b), hydrothermal synthesis (Gates *et al* 2000), and chemical synthesis (Huczko 2000). However, most of the above methods suffer from several serious limitations e.g. the conventional nanolithographic techniques are very cumbersome and require lot of efficiency and skill. Moreover, the techniques are also not suitable for large-scale production of nanowires with high aspect ratios (Das *et al* 1993; Sellmyer *et al* 2001). The hydrothermal and chemical synthesis techniques on the other hand are less attractive due to the difficulty in exercising control over the length and diameter of the nanowires during synthesis. Probably for the above reason, template based synthesis of nanowires and nanorods have recently gained lot of importance and popularity (Ozin 1992; Ying 1999).

Self-ordered nanoporous membrane of molecular sieves (Ozin 1992), track-etched polymer (Martin 1994), nanochannel array glass (Tonucci *et al* 1992), radiation track-etched mica (Possin 1970) and anodic aluminium oxide (AAO) (Furneaux *et al* 1989) are increasingly being used as the mask or the template for the nanowire fabrication. However, among the above mentioned templates AAO membrane is considered to be the most attractive due to the regular pore distribution, high pore density and high aspect ratio of pores (Routkevitch *et al* 1996a).

The AAO templates can be fabricated easily and during fabrication precise control can be exerted over the distribution, length and diameter of the pores. The AAO membranes are prepared by controlled electrochemical anodization, which involves oxidation of pure aluminium in an appropriate electrolyte. Anodization parameters such as anodization voltage, current, electrolyte bath temperature and

composition are all suitably adjusted during fabrication of the template to obtain the desired distribution, size and length of the pores (Masuda *et al* 1997). It would be worthwhile to mention that by using different electrochemical deposition methods (Doremus *et al* 1958) or by other processes such as evaporation, sol–gel method (Lakshmi *et al* 1997), chemical vapour deposition (CVD) (Lee *et al* 2001), melt or solution deposition (Zhang *et al* 1999; Han *et al* 2000) and electroless deposition (Mallory and Hadju 1990; Wu and Bein 1994), nanowires of different metals and semiconductor can be fabricated in the pores of this template membrane.

Considering the importance of the above aspects in the backdrop, herein we present a detailed review on the fabrication of nanowires by using the porous anodic aluminium oxide template.

2.1 *Preparation of AAO template*

A thick porous aluminium oxide film can be produced on the pure (99·999%) annealed aluminium by electrochemical anodization technique (Keller *et al* 1953). Anodization is an electrolytic oxidation process in which the metal surface, when anodic is converted primarily to an adherent oxide coating having desirable thickness and structure. Oxide layers with different morphological features can be formed by anodic oxidation of aluminium by varying the conditions during the electrochemical process, e.g. temperature, current density, voltage and duration of anodization. Therefore, we feel that it is imperative to include a brief description of the AAO template preparation.

2.1a *Surface preparation prior to anodization*: High purity Al foil (99·999% purity) is used for obtaining an ordered porous oxide film on aluminium by anodization, because of the fact that the impurity atoms having different size and volume may induce internal stresses during anodization, which can lead to the formation of defective structures in porous alumina template. It is also important that the Al foil should be annealed for atleast 3–4 h at 500°C under nitrogen atmosphere, which helps in the removal of crystal defects and promotes grain growth. A grain size between 100 and 200 μm is desirable for obtaining a uniform pore distribution during anodization (Jessensky *et al* 1998a).

Al foil with a thickness > 100 μm is cleaned in acetone prior to anodization by ultrasonic vibration. Surface impurities are removed by immersing the cleaned Al foil in a solution containing 1% HF, 10% HNO_3, 20% HCl, and 69% H_2O by volume (Li *et al* 1998).

The surface roughness of the annealed Al surface is reduced to nearly 3 nm (Li *et al* 1998) by electropolishing the aluminium foil in a standard acidic electrolyte containing 165 ml of 65% $HClO_4$, 700 ml of ethanol, 100 ml of 2-butoxyethanol and 137 ml of H_2O at 50 V for 10 s.

2.1b *Anodization of aluminium*: The electropolished Al sample is anodized in an electrochemical bath using the sample as anode plate and Pt mesh, graphite, Al or stainless steel as the cathode. Aqueous sulfuric, oxalic or phosphoric acid is used as an electrolyte (Diggle *et al* 1969; Despic and Parkhuitik 1989). During anodization, a thick porous alumina layer gradually grows over a very thin dense barrier oxide layer, which acts as an interface between the pure Al surface and porous alumina oxide layer. Here it is to be noted that pure Al and few other metals like Nb, W, Zr etc which are prone to oxidation under ambient condition develops a thin amorphous, insulating and inert oxide layer on the metal surface commonly known as the barrier oxide layer. The average thickness of this barrier layer ranges between 150 and 180 Å (Martin 1996).

It is also worthwhile to mention that for the preparation of ideally ordered porous structure the process parameters such as anodization voltage, anodization current, electrochemical bath temperature, type and concentration of electrolyte should be critically maintained.

Different types of electrolytic baths are used for the anodization. Some examples are: anodization using 0·3M $(COOH)_2$ solution at 1°C for 2–4 h with an anodization voltage between 30 and 40 V (Masuda and Fukuda 1995). Anodization can also be carried out by using 20 wt% (2 M) H_2SO_4 at 1°C with an applied voltage of 19 V for 1–2 days (Habib 2001) or 1 M H_3PO_4 under an applied voltage of 160 V for more than one day at low temperature in the range 1–10°C (Bocchetta *et al* 2003).

The pore diameter, cell dimension, pore distribution etc strongly depend on the applied voltage. In the anodization process the role of the anodization current is also considered to be very important. The current densities during the porous oxide film growth using 15% wt/vol. H_2SO_4 with bath temperatures of 20°C, 25°C and 30°C are 5, 15 and 35 mA/cm^2, respectively (Patermarakis and Papandreadis 1993). Since the conductivity and pH values of different electrolytes are different and are influenced by the concentration, ranges of anodization voltage are also different for different electrolytes. However, in all the cases the anodization temperature is purposely kept low, preferably below the room temperature because, high bath temperature enhances the dissolution of porous oxide film in the electrolyte.

Masuda and Satoh (1996) reported that rather than one-time (single step) anodization, two-step anodization is helpful in producing the ideally ordered porous structure. In the first step, Al is oxidized in 0·3 M oxalic acid at 40 V at low temperature, below room temperature for 15 min. The porous oxide layer so formed over the Al sample is removed by chemical etching in a mixture of 0·2 M chromic acid and 0·4 M phosphoric acid at a bath temperature of 60°C (Sellmyer *et al* 2001). Removal of the porous film from the Al sample leaves behind an ordered concave textured structure on the sample surface. This 'textured' Al is again anodized in the same electrolyte for a day or

more. During this second step anodization process, the concave textured pattern on the aluminium sample surface acts as the sites for deep pore growth and is helpful in growing the porous oxide film uniformly (Masuda *et al* 1997).

A pre-textured Al sample can also be used to fabricate uniformly ordered alumina oxide film (Masuda *et al* 1997) by anodization. In this method, a hexagonally ordered convex pattern is produced on the hard SiC using electron beam lithography technique. This patterned SiC is used as the master mould. This SiC mould is indented into the Al sample surface at high pressure (~2800 kg/cm^2) before anodization is carried out. This process helps to get an ideally distributed shallow order concave pattern on the Al sample surface (Asoh *et al* 2001). When the sample is anodized, the shallow ordered concave patterns act as the site for deep pore growth with uniform, similar morphological and geometrical features.

2.1c *Mechanism of pore growth and reactions*: During the anodization process a constant voltage is applied between the electrodes. Therefore, the applied electric field lines lie perpendicular to the sample surface (anode) towards the cathode. This applied electric field increases the dissolution of the barrier oxide layer and thus favours pore growth. Due to the competition that prevails among the growing pores, few of them stop growing while others grow. The pores grow perpendicular to the surface when the field-enhanced dissolution of the oxide at the electrolyte/oxide interface is equilibrated with the growth of oxide that occurs at the oxide/metal interface. Oxidation occurs at the metal/oxide interface by the migration of oxygen containing ions (O^{2-} or OH^-) from the electrolyte by the following reaction (Uchi *et al* 2001)

$$2Al + 3O^{2-} \rightarrow Al_2O_3 + 6e^-.$$

Dissolution of the oxide layer is caused mainly by the hydration reaction of the formed oxide layer as shown below (Alwitt and Takei 1983; Xu *et al* 1985; Shimizu *et al* 1992)

$$2Al^{3+} + 3H_2O \rightarrow Al_2O_3 + 6H^+.$$

It is to be noted that under the applied electric field the Al^{3+} ions migrate through the barrier oxide layer. This electric field also helps in the transport of the oxygen containing ions (O^{2-} or OH^-) from the electrolyte into the barrier oxide layer towards the Al substrate. The schematic representation of the ionic migration at the pore bottom under the applied electric field is given in figure 21. The electrons ejected into the electrolyte and combined with hydrogen ions to generate hydrogen gas at cathode (Thompson and Wood 1983).

Barrier oxide growth without pore formation occurs when the Al^{3+} ions reach the electrolyte/oxide interface and contribute to the oxide formation. Porous alumina oxide layer formed when the Al^{3+} ions drift through the oxide layer and are ejected into the solution at the oxide/electrolyte interface (Shimizu *et al* 1992)

$$2Al \rightarrow 2Al^{3+} + 6e^-.$$

Loss of Al^{3+} ions in the electrolyte has been found to be a prerequisite for porous oxide growth. Thus at steady state pore grows perpendicular to the Al surface when an equilibrium is established between the field enhanced dissolution of oxide layer at oxide/electrolyte interface and the oxide growth at metal/oxide interface (O'Sullivan and Wood 1970; Parkhutik and Shershulsky 1992).

During the anodization of aluminium, the porous layer formed is assumed to be of Al_2O_3. The atomic density of aluminium in Al_2O_3 is lower than that of metallic aluminium by a factor of two. The volume expansion of Al_2O_3 will be nearly twice that of the original aluminium metal. This volume expansion takes place at the metal/oxide interface leading to a compressive stress during oxide formation. This stress is the origin of the repulsive forces that appear between the neighbouring pores (Jessensky *et al* 1998b) and it is believed that volume expansion in the vertical direction pushes the pore wall upward.

2.1d *Morphology and geometrical structure of porous aluminium oxide*: Atomic force microscopic (AFM) techniques are commonly used to show the three-dimensional surface topology of the porous film and scanning tunneling microscopic (STM) image gives an idea about the geometrical structure in real space. It has been found that depending on certain sets of parameters e.g. composition of the electrolyte, applied voltage etc, the pore diameter ranges from 4–200 nm, pore length from 1–50 μm and pore density in the range of 10^9–10^{11}/cm^2 (Routkevitch *et al* 1996a).

It has been seen that the porous anodic alumina produced during anodization, have hexagonal closed packed

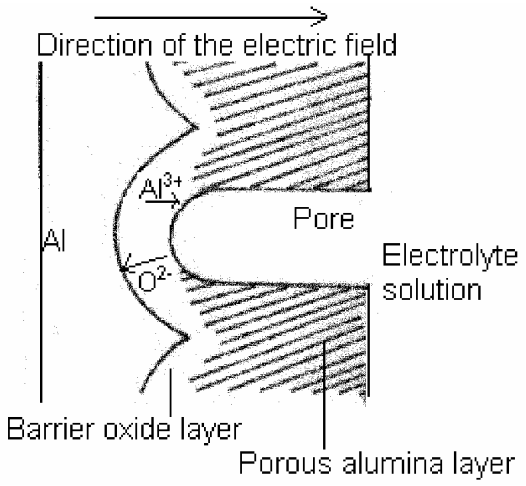

Figure 21. Schematic showing the ionic migration under applied electric field.

nearly honeycomb like structure as shown in figure 22. The pores appear nearly at the centre of each hexagonal columnar cell. The channel like pores lie perpendicular to the aluminium sample surface (Jessensky *et al* 1998b). However, the geometry of AAO film usually obtained by anodization process is far from that of the idealized model as the arrangement of the cells is not perfectly hexagonal (see figure 23) (O'Sullivan and Wood 1970).

2.2 *Fabrication of nanowires by pore filling through electro-deposition technique*

Methods that involve direct pore filling of the AAO template are considered to be straightforward and versatile techniques for synthesizing nanowires. Highlights of some of the AAO pore filling techniques that have gained reasonable popularity are described below.

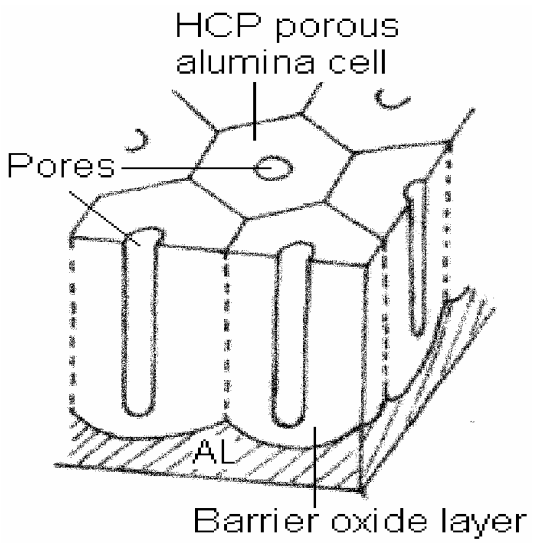

Figure 22. Schematic diagram showing the honeycomb like porous alumina structure.

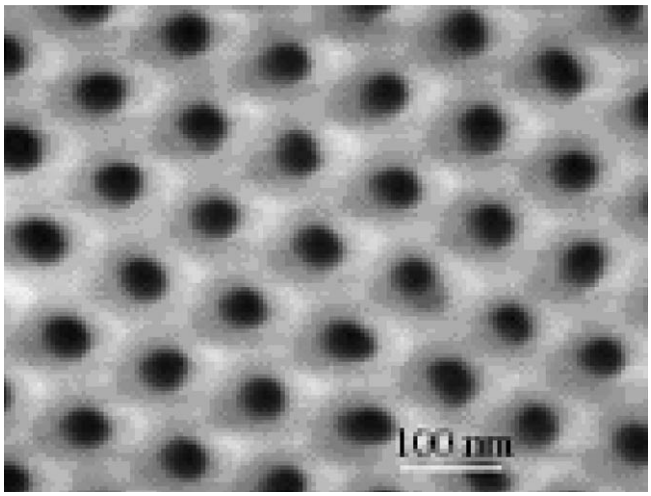

Figure 23. SEM image of the top surface of AAO membrane (Heremans *et al* 1998).

2.2a *Pressure injection*: In this technique low melting point metals and semiconductors are melted and injected into the pores of AAO template by applying high pressure. The material that has infiltrated into the pores is allowed to solidify and form nanowires. The nanowires were finally extracted by dissolving the alumina template chemically. Nanowires of Bi, Sn, In, Al, Te, Se, GaSb and Bi_2Te_3 have been reportedly fabricated by this technique (Huber *et al* 1994; Zhang *et al* 1998b).

2.2b *Vapour deposition*: Physical and chemical vapour deposition techniques are often employed for pore filling and fabricating nanowires. Bi nanowires in AAO template have been synthesized by introducing Bi vapour into the pores of the AAO template, which is then solidified by cooling (Heremans *et al* 2000). Compound semiconductor nanowires of GaN have also been reportedly synthesized in AAO template by gas phase reaction between Ga_2O vapour and ammonia (Cheng *et al* 1999).

2.2c *Vapour–liquid–solid (VLS) method*: This method involves absorption of source material from the gaseous phase into a liquid droplet that acts as a catalyst. Primarily a liquid alloy is formed which becomes supersaturated and precipitates out the source material by nucleation. The precipitate acts as a preferred site for further deposition and growth of the material at the interface of the liquid droplet, favouring growth of the precipitate into a nanowire by suppressing further nucleation on the same catalyst. It has been shown that the diameter of the nanowire depends on the diameter of the liquid alloy droplet. Recently, porous alumina membrane has been used as an alternative to control nanowire diameter in the VLS process (Lew *et al* 2002; Bogart *et al* 2005). Defect free Si nanowires with diameters in the range of 4–5 nm and lengths of several microns were synthesized by using a supercritical fluid solution phase approach where alkanethiol coated Au nanocrystal (2·5 nm in diameter) were used as seeds to direct the one dimensional crystallization of Si in a solvent heated and pressurized above its critical point (Holmes *et al* 2000). The reaction pressure controls the orientation of the nanowires.

2.2d *Pulsed laser deposition*: Recently, pulsed laser deposition (PLD) technique is being used to deposit materials on top of the porous AAO template. The material deposited inside the pores is shaped into nanowires and the material that is deposited in the nonporous region that separate adjacent pores, assume different morphologies depending on the nature of the surface. It has been reported that ordered arrays of ZnO nanodots with an average diameter of 60 nm and a periodicity of 100 nm were

fabricated by PLD using AAO template. Controlling the oxygen pressure used in PLD photoluminescence (PL) at 380 nm is observed from the ZnO nanodots (Bae *et al* 2006).

2.2e *Chemical conversion*: Synthesis of nanowires by chemical reaction in the pores of AAO template is another important approach. Initially nanowires of the constituent element is prepared, which is then reacted with chemicals containing the desired element to form the final product. Ag_2Se nanowires were synthesized by reacting crystalline Se nanowires with aqueous $AgNO_3$ at room temperature (Ma *et al* 2002).

ZnO nanowires were prepared by oxidizing metallic zinc nanowires that were prepared by electrodeposition in the pores of AAO template prior to their oxidation in air at 300°C for 35 h. The free standing ZnO nanowires were extracted from the template by selective dissolutions (Li *et al* 2000).

Hollow nanotubes of MoS_2 ~30 nm long with 50 nm external diameters were prepared by filling the pores of the AAO template with a mixture of molecular precursors, $(NH_4)_2MoS_4$ and $(NH_4)_2Mo_3S_{13}$. The filled template was then heated at an elevated temperature to thermally decompose the precursor into MoS_2 (Zelenski and Dorhout 1998).

2.2f *Colloidal dispersion filling*: Oxide nanowires, nanorods and nanotubes can be synthesized easily by filling the template with colloidal dispersions. The colloidal dispersion was generally prepared through the sol–gel technique. The porous template was placed in a stable sol for appropriate length of time to drive the sol into the pores by capillary force. The filled template is then withdrawn from the sol and dried prior to firing for densification of the sol–gel derived nanowires, nanorods or nanotubes (Lakshmi *et al* 1997).

2.2g *Electro-deposition method*: Inspite of the fact that all the above mentioned techniques are advantageously used for the deposition of nanostructure materials (NSMs) into the pores of the nanoporous membrane, electrodeposition or electrochemical deposition is regarded as one of the most popular methods of pore filling with conducting metals to obtain continuous arrays of nanowires with large aspect ratios (Huixin and Nongjian 2003). Electrochemical deposition route is easy, low-cost as well as less skill dependent compared to other techniques mentioned above. Structural analysis shows that the electrodeposited nanowires tend to be densely packed, continuous and highly crystalline. Moreover, by simply monitoring the total amount of passing charge one can precisely control the aspect ratios of the metal nanowires.

2.2g(i) *Electro-deposition bath set up*: In the electrodeposition method the electrochemical bath set up is similar to that used for the electro-plating process. The porous alumina membrane with natural aluminium-substrate support is used as the electrode. Sometimes the anodic alumina oxide (AAO) membrane is separated out from the Al-substrate and a thin metal film of Ag or Au is deposited in the membrane by evaporation technique (Mikhaylova *et al* 2002). This thin metal film supported membrane acts as the active electrode. The appropriate metal salt solution, containing the metal ions is used as the electrolyte in the electro-deposition process.

2.2g(ii) *Electro-deposition method*: The thin barrier oxide layer underneath the pores of AAO membrane has high resistivity (10^{10}–10^{12} Ωcm) (Linden *et al* 1990). A.C. electrodeposition technique is preferred because direct current cannot pass through the barrier oxide layer (Lee *et al* 2002; Zeng *et al* 2002). Electro-deposition depends on different process parameters such as deposition current amplitude, frequency of current (voltage), electrochemical bath temperature and pH value of the electrolyte (Rahman *et al* 2003). In a.c. electrodeposition the anodic alumina template acts like a 'rectifier' when alternating current (voltage) is applied between the template and other electrodes. The ionic conduction starts when the template electrode acts as a cathode (during cathodic half cycle). Under this condition the cations from the electrolyte layer that remain attached to the template electrode diffuse to the pore bottom and are electrodeposited. On the other hand, while the template becomes anodic (during anodic half cycle), ionic conduction is cut off and the material deposited in the pore bottom of the membrane is not re-anodized. Here, it is to be noted that during the cathodic half cycle the electrolyte layer, which is attached to the template electrode becomes depleted of cation, as the ion diffusion from the rest of the electrolyte to this thin attached layer is very slow. Therefore, the anodic half cycle is helpful in the sense that during this interval or period cations get the time to diffuse into the thin electrolyte layer, from rest of the electrolyte solution making electro-deposition possible during the next cathodic half cycle.

Here, it would be worthwhile to mention that d.c. pulsed electro-deposition can also be used for pore filling, however, this process has the ability to fill-up only 10–20% of the pores of the membrane (Prieto *et al* 2001). On the other hand, a.c. electro-deposition is capable of high pore filling ratio (Nielsch *et al* 2000; Sauer *et al* 2002; Seadi and Ghorbani 2005).

2.2g(iii) *Electro-deposition of nanowires*: Metallic nanowires of Cu (Blondel *et al* 1994; Piraux *et al* 1994), Ag (Bhattacharrya *et al* 2000; Sauer *et al* 2002), Bi (Liu *et al* 1998; Piraux *et al* 1999), Au (Hornyak *et al* 1997; Zhang *et al* 2001) and different transition metals such as Fe (Al Mawlawi *et al* 1991; Peng *et al* 2000), Co (Ferré *et al* 1997; Zeng *et al* 2000), Ni (Ferré *et al* 1997; Sun *et al*

1999) and their alloys can be fabricated by the electrodeposition method by filling the pores of the alumina template. Nanowires of different semiconductors, superlattice and superconductors such as Pb (Yi and Schwarzacher 1999) can also be fabricated. Representative SEM image of silver nanowires fabricated in alumina template by electrodeposition is shown in figure 24 (Riveros *et al* 2006).

It has been reported that Fe nanowires are deposited into the pores of the template by using a.c. pulse. The electrolyte solution contains 120 g/l of $FeSO_4{\cdot}7H_2O$; 45 g/l of H_3PO_3; 1 g/l of ascorbic acid and 2 ml/l of glycerin. The pH value of the solution was maintained at ≈ 3 throughout the electrodeposition process (Hickmott 2000). Similarly, Co nanowires were fabricated from $CoSO_4$ salt solution containing 400 g/l of $CoSO_4{\cdot}7H_2O$ and 40 g/l of H_3BO_4 as electrolyte (Mikhaylova *et al* 2002). In both the Fe and Co electro-deposition processes, a.c. voltage pulse of 10–20 V with frequency ranging from 50–300 Hz was used (Menon *et al* 2000). It has also been reported that by using highly concentrated electrolyte like 300 g/l $NiSO_4{\cdot}6H_2O$ or 45 g/l $NiCl_2{\cdot}6H_2O$ and 45 g of H_3BO_4 solution of pH 4·5 (Nielsch *et al* 2001), Ni nanowires can be deposited into the pores of the alumina template under a negative current pulse of –25 mA/cm^2 for a duration of 6 ms followed by a positive voltage pulse of +4 V for 2 ms only (Nielsch *et al* 2001). Semiconductor nanowires of CdS (Routkevitch *et al* 1996b) have been fabricated by electrodeposition method using the alumina oxide template. It has been reported (Xu D *et al* 2000; Xu D S *et al* 2000) that single crystal compound semiconductor nanowires of CdS, CdSe and CdTe can also be fabricated into the porous alumina template by electrodeposition.

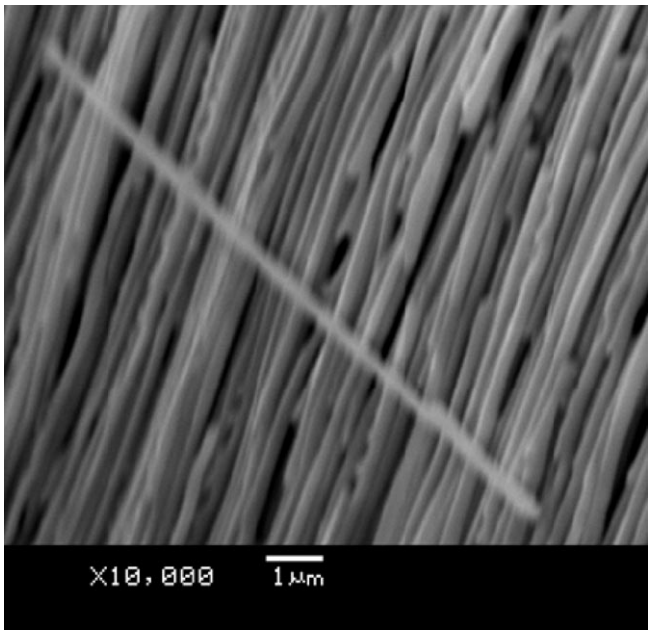

Figure 24. SEM image of Ag nanowires separated from the alumina template (Riveros *et al* 2006).

Xu D *et al* (2000) and Xu D S *et al* (2000) reported that Co–Cu superlattice nanowires can also be synthesized by varying the cathodic potential in the electrolyte solution containing two different metal ions. These nanowires contain periodic modulation of composition along the wire axes. Here it would be worthwhile to mention that after pore filling with required materials, the aluminium substrate was removed by $HgCl_2$ solution (Terry *et al* 2003). The periodic arrays of nanowires may be separated out of the template by dissolving AAO membrane in hot 6 M NaOH solution (Terry *et al* 2003).

3. Conclusions

In the present review article, physical properties of the nanowires along with their potential applications are described in detail. It is concluded that (i) nanowires possess physical and chemical properties that are unique and often conspicuously different from their bulk parent counterparts and (ii) nanowires are potential candidates for different nanoscale electrical, thermoelectrical, optical, magnetic, bio-medical and sensor device applications.

The review has also established that synthesis of nanowires via AAO template is very attractive due to the uniform pore morphology and high pore density. Moreover, the technique is reliable, simple and economical.

Acknowledgements

Authors are thankful to the Department of Science and Technology, New Delhi, for providing financial support through the fast track scheme (ref no-SR/FTP/CS-8/2004) for the work. The authors are also thankful to Nature Publishing Group, Wiley-VCH, IOP Publishing Limited, American Institute of Physics and Royal Society of Chemistry for their permission to use some of the published figures in this review.

References

Aldén M, Skriver H L, Mirbt S and Johansson B 1994 *Surf. Sci.* **315** 157

Al Mawlawi D, Coombs N and Moskovits M 1991 *J. Appl. Phys.* **70** 4421

Alwitt R S and Takei H 1983 *Thin Films Sci. & Technol.* **4** 741

Asoh H, Nishio K, Nakao M, Tamamura T and Masudaa H 2001 *J. Electrochem. Soc.* **148** B152

Aspnes D E 1982 *Thin Solid Films* **89** 249

Au F C K, Wong K W, Tang Y H, Zhang Y F, Bello I and Lee S T 1999 *Appl. Phys. Lett.* **75** 1700

Bae C H, Park S M, Park S C and Ha J S 2006 *Nanotechnology* **17** 381

Beck G, Petrikowski K and Khan H R 2005 *Conf. on microstructure analysis in materials science* (TU Bergakademie Freiberg: Leitung und Zentrales Tagungsbüro)
Beutler D E and Giordano N 1988 *Phys. Rev.* **B38** 8
Bhattacharrya S, Saha S K and Chakravorty D 2000 *Appl. Phys. Lett.* **76** 3896
Bhushan B (ed.) 2005 *Springer handbook of nanotechnology* (Berlin, Heidelberg: Springer)
Björk M T, Ohlsson B J, Thelander C, Persson A I, Deppert K, Wallenberg L R and Samuelson L 2002a *Appl. Phys. Lett.* **81** 4458
Björk M T, Ohlsson B J, Sass T, Persson A I, Thelander C, Magnusson M H, Deppert K, Wallenberg L R and Samuelson L 2002b *Nano. Lett.* **2** 87
Black M R, Lin Y M, Cronin S B, Rabin O and Dresselhaus M S 2002 *Phys. Rev.* **B65** 195417
Blom S, Gorelik L Y, Jonson M, Shekhter R I, Scherbakov A G, Bogachek E N and Landman U 1998 *Phys. Rev.* **B58** 16305
Blondel A, Meier J P, Doudin B and Ansermet J P 1994 *Appl. Phys. Lett.* **65** 3019
Bocchetta P, Sunseri C, Masi R, Piazza S and Quarto F D 2003 *Mater. Sci. & Eng.* **C23** 1021
Bogart T E, Dey S, Lew K -K, Mohney S E and Redwing J M 2005 *Adv. Mater.* **17** 114
Bohreu C F and Huffman D R 1983 *Absorption and scattering of light by small particle* (New York: Wiley)
Cardona M 1982 *Light scattering in solids* (Berlin, Heidelberg: Springer)
Cerrina F and Marrian C 1996 *MRS Bull.* **21** 56
Chatterjee K, Basu S and Chakravorty D 2006 *Mater. Res. Soc.* **21** 34
Chen G, Dresselhaus M S, Dresselhaus G, Fluerial J P and Caillat T 2003 *Int. Mater. Rev.* **48** 45
Cheng G S, Zhang L D, Zhu Y, Fei G T, Li L, Mo C M and Mao Y Q 1999 *Appl. Phys. Lett.* **75** 2455
Chien C L 1991 *J. Appl. Phys.* **69** 5267
Chou S Y, Wei M, Krauss R P and Fisher B P 1994 *J. Vac. Sci. Technol.* **B12** 3695
Chung S W, Yu J Y and Heath J R 2000 *Appl. Phys. Lett.* **76** 2068
Costa-Krämer J L, Garcia N and Olin H 1997 *Phys. Rev. Lett.* **78** 4990
Cui Y, Duan X, Hu J and Lieber C M 2000 *J. Phys. Chem.* **B104** 5213
Cui Y, Wei Q, Park H and Lieber C 2001 *Science* **293** 1289
Dames C and Chen G 2002 *21st Int. conf. thermoelectrics: Proc. ICT symposium, Long Beach* (Piscataway: IEEE) pp 317–320
Das B, Subramanium S and Melloch M R 1993 *Semicond. Sci. Technol.* **8** 1347
Derycke V, Martel R, Appenzeller J and Avouris P 2001 *Nano Letts* **1** 453
Despic A and Parkhuitik V P 1989 *Modern aspects of electrochemistry* (New York: Plenum) Vol. 20
Diggle J W, Downie T C and Goulding C W 1969 *Chem. Rev.* **69** 365
Ding M, Kim H and Akinwande A I 1999 *Appl. Phys. Lett.* **75** 823
Doremus R H, Roberts B W and Turnbull D 1958 *Growth and perfection of crystal* (New York: John Wiley) p. 13
Dresselhaus G, Dresselhaus M S, Zhang Z, Sun X, Ying J and Chen G 1998 *17th Int. conf. thermoelectrics: Proc. ICT'98, Nagoya* (ed.) K Koumoto (Piscataway: Institute of Electrical and Electronics Engineers Inc) pp 43–46
Duan X, Huang Y, Cui Y, Wang J and Lieber C M 2001 *Nature* **409** 66
Duan X, Huang Y and Lieber C M 2002 *Nano. Lett.* **2** 487
Dunn P N 1994 *Solid State Technol.* **37** 49, 52, 58, 61
Favier F, Walter E C, Zach M P, Benter T and Penner R M 2001 *Science* **293** 2227
Ferré R, Ounadjela K, George J M, Piraux L and Dubois S 1997 *Phys. Rev.* **B56** 14066
Foss C A, Hornyak G L, Stocket J A and Martin C R 1994 *J. Phys. Chem.* **98** 2963
Furneaux R C, Rigby W R and Davidson A P 1989 *Nature* **337** 147
Garnett J C M 1906 *Philos. Trans. R. Soc. London* **A205** 237
Gates B, Yin Y and Xia Y 2000 *J. Am. Chem. Soc.* **122** 12582
Gibson J M 1997 *Phys. Today* 56
Gudiksen M S, Lauhon L J, Wang J, Smith D C and Lieber C M 2002 *Nature* **415** 617
Habib K 2001 *Corros. Sci.* **43** 449
Han Y J, Kim J M and Stucky G D 2000 *Chem. Mater.* **12** 2068
Hasegawa H 2001 *ECS 2001 joint international meeting, 6th International symposium on quantum confinement* (San Francisco, California: The International Society of Electrochemistry)
Hehn M, Ounadjela K, Bucher J, Rousseaux F, Deeanini D, Bartenlian B and Chappert C 1995 *Science* **272** 1782
Heremans J and Thrush C M 1999 *Phys. Rev.* **B59** 12579
Heremans J, Thrush C M, Zhang Z, Sun X, Dresselhaus M S, Ying J Y and Morelli D T 1998 *Phys. Rev.* **B58** R10091
Heremans J, Thrush C M, Lin Y M, Cronin S, Zhang Z, Dresselhaus M S and Mansfield J F 2000 *Phys. Rev.* **B61** 2921
Heremans J, Thrush C M, Morelli D T and Wu M C 2002 *Phys. Rev. Lett.* **88** 216801
Hickmott T W 2000 *J. Appl. Phys.* **87** 11
Hicks L D and Dresselhaus M S 1993 *Phys. Rev.* **B47** 16631
Holmes J D, Johnston K P, Doty R C and Korgil B A 2000 *Science* **287** 1471
Hornyak G L, Patrissi C J and Martin C M 1997 *J. Phys. Chem.* **B101** 1548
Huang H H, Ni X P, Loy G L, Chew C H, Tan K L, Loh F C, Deng J F and Xu G Q 1996 *Langmuir* **12** 909
Huang M H *et al* 2001a *Science* **292** 1897
Huang M H *et al* 2001b *Adv. Mater.* **13** 113
Huang Y, Duan X, Cui Y, Lauhon L J, Kim K H and Lieber C 2001 *Science* **294** 1313
Huang Y, Duan X, Cui Y and Lieber C M 2002 *Nano. Lett.* **2** 101
Huang Y, Duan X and Lieber C M 2005 Wiley-VCH Verlag GmbH & Co. KGaA, D-69451 Weinheim
Huber C A, Huber T E, Sadoqi M, Lubin J A, Manalis S and Prater C B 1994 *Science* **263** 800
Huczko A 2000 *Appl. Phys.* **A70** 365
Huixin H and Nongjian J T 2003 *Encyclopedia of nanoscience and nanotechnology* (ed.) H S Nalwa (Valencia, California, USA: American Scientific Publishers) **Vol. 10**, pp 1–18
Huynh W U, Dittmer J J and Alivisatos A P 2002 *Science* **295** 2425
Jessensky O, Muller F and Gosele U 1998a *Appl. Phys. Lett.* **72** 1173

Jessensky O, Muller F and Gosele U 1998b *J. Electrochem. Soc.* **145** 3735
Jiang X, Xie Y, Lu J, Zhu L, He W and Qian Y 2001 *J. Mater. Chem.* **11** 1775
Johnson J C, Yan H, Schaller R D, Haber L H, Saykally R J and Yang P 2001 *J. Phys. Chem.* **B105** 11387
Johnson J C, Choi H J, Knutsen K P, Schaller R D, Yang P and Saykally R J 2002 *Nature Mater.* **1** 106
Keller F, Hunter M S and Robinson D L 1953 *J. Electrochem. Soc.* **100** 411
Kerker M 1969 *Scattering of light and other electromagnetic radiation* (New York: Academic Press)
Kim J R, Oh H, So H M, Kim J J, Kim J, Lee C J and Lyu S C 2002 *Nanotechnology* **13** 701
Lakshmi B B, Dorhout P R and Martin C R 1997 *Chem. Mater.* **9** 857
Lauhonn L J, Gudiksen M S, Wang D and Lieber C M 2002 *Nature* **420** 57
Lee K B, Lee S M and Cheon J 2001 *Adv. Mater.* **13** 517
Lee K H, Lee H Y, Jeung W Y and Lee W Y 2002 *J. Appl. Phys.* **91** 8513
Lee M W, Twu H Z, Chen C C and Chen C H 2001 *Appl. Phys. Lett.* **79** 3693
Lew K -K, Reuther C, Carim A H and Recluring J M 2002 *J. Vac. Sci. Technol.* **B20** 389
Li A P, Muller F, Birner A, Nielseh K and Gosele U 1998 *J. Appl. Phys.* **84** 6023
Li Y, Cheng G S and Zhang L D 2000 *J. Mater. Res.* **15** 2305
Lin Y M and Dresselhaus M S 2002 *MRS symp. proc. Boston* (eds) J M Buriak *et al* (Boston: Materials Research Society Press) **737** p. F8.18
Lin Y M and Dresselhaus M S 2003 *Phys. Rev.* **B68** 075304
Lin Y M, Sun X and Dresselhaus M S 2000 *Phys. Rev.* **B62** 4610
Lin Y M, Rabin O, Cronin S B, Ying J Y and Dresselhaus M S 2002 *Appl. Phys. Lett.* **81** 2403
Linden B V, Terryn H and Vereehen J 1990 *J. Appl. Electrochem.* **20** 798
Liu F, Press M R, Khanna S N and Jana P 1989 *Phys. Rev.* **B39** 6914
Liu K, Chien C L, Searson P C and Kui Y Z 1998 *Appl. Phys. Lett.* **73** 1436
Liu Y, Zheng C, Wang W, Yin C and Wong G 2001 *Adv. Mater.* **13** 1883
Lyons D M, Ryan K M, Morris M A and Holmes J D 2002 *Nano. Lett.* **2** 811
Ma X D, Qian X F, Yin Z and Zhu Z K 2002 *J. Mater. Chem.* **12** 663
Maier S A, Kik P G and Atwater H A 2002 *Appl. Phys. Lett.* **81** 1714
Maier S A *et al* 2003 *Nature Mater.* **2** 229
Mallory G O and Hadju J B 1990 *Electroless plating: Fundamentals and applications* (Orlando, FL: American Electroplates and Surface Finishing Society)
Martin C R 1994 *Science* **266** 1961
Martin C H 1996 *Chem. Mater.* **8** 1739
Masuda H and Fukuda K 1995 *Science* **268** 1466
Masuda H and Satoh M 1996 *Jap. J. Appl. Phys.* **L126** 1135
Masuda H, Hasegawa F and Ono S 1997 *J. Electrochem. Soc.* **144** L127
Masuda H, Yamada H, Satoh M, Asoh H, Nakao M and Tamamura T 1997 *Appl. Phys. Lett.* **71** 19
Matsui S and Ochiai Y 1996 *Nanotechnology* **7** 247
Melle S, Menéndez J L, Armelles G, Navas D, Vázquez M, Nielsch K, Wehrspohn R B and Gosele U 2003 *Appl. Phys. Lett.* **22** 83
Menon L, Zeng M, Zeng H, Bandyopadhyay S and Sellmyer D J 2000 *J. Electron. Mater.* **29** 510
Mikhaylova M, Toprak M, Kim D K, Zhang Y and Muhammed M 2002 *Mater. Res. Soc. Symp. Proc.* **704** W6.34.1
Molaresa M E *et al* 2003 *Appl. Phys. Lett.* **82** 13
Muller C J, van Ruitenbeek J M and de Jongh L J 1992 *Phys. Rev. Lett.* **69** 140
Muller C J, Krans J M, Todorov T N and Reed M A 1996 *Phys. Rev.* **B53** 1022
Nicewarner Pena S R *et al* 2004 *Encyclopedia of nanoscience and nanotechnology* (Valencia, California, USA: American Scientific Publishers) **Vol. 6**, p. 215
Nielsch K, Muller F, Li A P and Gosele U 2000 *Adv. Mater.* **12** 582
Nielsch K, Wehrspohn R B, Fischer S F, Kronmiller H, Kirsehner J and Gosele U 2001 *Mater. Res. Soc. Symp. Proc.* **9** 636
O'Sullivan J P and Wood G C 1970 *Proc. R. Soc. London* **A317** 511
Ozin G A 1992 *Adv. Mater.* **4** 612
Parkhutik V P and Shershulsky V I 1992 *J. Phys. D: Appl. Phys.* **25** 1258
Patermarakis G and Papandreadis N 1993 *Electrochim. Acta* **38** 1413
Peng Y, Zhang H L, Pan S L and Li H L 2000 *J. Appl. Phys.* **87** 7405
Peng Y, Shen T H and Ashworth B 2003 *J. Appl. Phys.* **93** 7050
Pierce J P, Plummer E W and Shen E 2002 *Appl. Phys. Lett.* **81** 1890
Piraux L, George J M, Despres J F, Leroy C, Ferain E, Legras R, Ounadjela K and Fert A 1994 *Appl. Phys. Lett.* **65** 2484
Piraux L, Dubois S, Duvail J L, Radulescu A, Demoustier-Champagne S, Ferain E and Legras R 1999 *J. Mater. Res.* **14** 3042
Possin G E 1970 *Rev. Sci. Instrum.* **41** 772
Prieto A L, Sander M S, Martin-Gonzalez M S, Gronsky R, Sands T and Stacy A M 2001 *J. Am. Chem. Soc.* **123** 7160
Rahman I Z, Razeeb K M, Rhaman M A and Kamruzzaman Md 2003 *J. Magn. & Magn. Mater.* **262** 166
Ratner M and Ratner D 2003 *Nanotechnology: A gentle introduction to the next big idea* (London: Pearson Education publication)
Redwing J, Mayer T, Mohney S and Mizel A 2002 *NSF nanoscale science and engineering grantees conference* (Arlington, Virginia: National Science Foundation)
Riveros G, Green S, Cortes A, Gomez H, Marotti R E and Dalchiele E A 2006 *Nanotechnology* **17** 561
Routkevitch D, Bigioni T, Moskovits M and Xu J M 1996a *J. Phys. Chem.* **100** 14037
Routkevitch D, Tager A A, Haruyama J, Al Mawlawi D, Moskovits M and Xu M J 1996b *IEEE Trans. Magn.* **43** 1646
Sauer G, Brehm G, Schneider S, Nielsch K, Wehrspohn R B, Choi J, Hofmeister H and Gösele U 2002 *J. Appl. Phys.* **91** 3243
Schider G, Krenn J R, Gotschy W, Lamprecht B, Ditlbacher H, Leitner A and Aussenegg F R 2001 *J. Appl. Phys.* **90** 3825
Schider G, Krenn J R, Hohenau A, Ditlbacher H, Leitner A and Aussenegg F R 2003 *Phys. Rev.* **B68** 155427

Seadi A and Ghorbani M 2005 *Mater. Chem. & Phys.* **91** 417
Sellmyer D J, Zheng M and Skomski R 2001 *J. Phys. Condens. Matter* **13** R433
Shimizu K, Kobayashi K, Thompson G E and Wood G C 1992 *Philos. Mag.* **A66** 643
Skomsk R, Zeng H and Sellmyer D J 2000 *Phys. Rev.* **B62** 3900
Spencer M J S, Hung A, Snook I K and Yarovsky I 2002 *Surf. Sci.* **513** 389
Sugawara A, Coyle T, Hembree G G and Scheinfein M R 1997 *Appl. Phys. Lett.* **70** 1043
Sun L, Searson P C and Chien C L 1999 *Appl. Phys. Lett.* **74** 2803
Takahara J, Yamagishi S, Taki H, Morimoto A and Kobayashi T 1997 *Opt. Lett.* **22** 475
Terry T, Xu R, Piner D and Rodney S 2003 *Langmuir* **19** 1443
Thompson G E and Wood G C 1983 *Treatise on materials science and technology* (New York: Academic Press) **Vol. 23**, pp 205–329
Thurn-Albrecht T *et al* 2000 *Science* **290** 2126
Tong L, Gattass R R, Ashcom J B, He S, Lou J, Shen M, Maxwell I and Mazur E 2003 *Nature* **426** 18
Tonucci R J, Justus B L, Campillo A J and Ford C E 1992 *Science* **258** 783
Uchi H, Kanno T and Alwitt R S 2001 *J. Electrochem. Soc.* **148** B17
van Vugt L K, Sandra J, Veen S J, Bakkers E P A M, Roest A L and Vanmaekelbergh D 2005 *J. Am. Chem.. Soc.* **127** 12357
van Wees B J, van Houten H, Beenakker C W J, Williamson J G, Kouvenhoven L P, van der Marel D and Foxon C T 1988 *Phys. Rev. Lett.* **60** 848
Venkatasubramanian R, Siivola E, Colpitts T and O'Quinn B 2001 *Nature* **413** 597
Vitos L, Ruban A V, Skriver H L and Kollár J 1998 *Surf. Sci.* **411** 186
Wanekaya A K, Chen W, Myung N V and Mulchandani A 2006 *Electroanalysis* **18** 533
Wang B, Yin S, Wang G and Zhao J 2001 *J. Phys.: Condens. Matter* **13** L403
Way Z L 2003 *Nanowires and nanobelts materials preparation and devices, metal and semiconductor nanowires* (Boston: Kluwer Academic Publication) **Vol. 1**
Wharam D A *et al* 1988 *J. Phys. C: Solid State Phys.* **21** L209
Whitney T W, Jiang J S, Searoon P C and Chien C L 1993 *Science* **261** 1316
Wu C G and Bein T 1994 *Science* **264** 1757
Wu Y and Yang P 2000 *Chem. Mater.* **12** 605
Wu Y, Fan R and Yang P 2002 *Nano. Lett.* **2** 83
Xu D, Xu Y, Chen D, Guo G, Gui L and Tang Y 2000 *Adv. Mater.* **12** 520
Xu D S, Chen D P, Xu Y J, Shi X S, Guo G L, Gui L L and Tang Y Q 2000 *Pure Appl. Chem.* **72** 127
Xu Y, Thompson G E and Wood G C 1985 *Trans. Inst. Met. Finish.* **63** 98
Yi G and Schwarzacher W 1999 *Appl. Phys. Lett.* **74** 1746
Ying I Y 1999 *Sci. Spectra* **18** 56
Yu P Y and Cardona M 1995 *Fundamentals of semiconductors* (Berlin, Heidelberg: Springer) Ch. 7
Zelenski C M and Dorhout P K 1998 *J. Am. Chem. Soc.* **120** 734
Zeng H, Zheng M, Skomski R, Sellmyer D J, Liu Y, Menon L and Bandyopadhyay S 2000 *J. Appl. Phys.* **87** 4718
Zeng H, Skomki R, Menon L, Liu Y, Bandyopadhyay S and Sellmyer D J 2002 *Phys. Rev.* **B65** 13426
Zhang X Y, Zhang L D, Lei Y, Zhao L X and Mao Y Q 2001 *J. Mater. Chem.* **11** 1732
Zhang Z, Sun X, Dresselhaus M S, Ying J Y and Heremans J 1998a *Appl. Phys. Lett.* **73** 1589
Zhang Z, Ying J Y and Dresselhaus M S 1998b *J. Mater. Res.* **13** 1745
Zhang Z, Gekhtman D, Dresselhaus M S and Ying J Y 1999 *Chem. Mater.* **11** 1659
Zhang Z, Sun X, Dresselhaus M S, Ying J Y and Heremans J 2000 *Phys. Rev.* **B61** 4850
Zheng M J, Zhang L D, Li G H and Chen W Z 2002 *Chem. Phys. Lett.* **363** 123
Zhao J, Buia C, Han J and Lu J P 2003 *Nanotechnology* **14** 501